ANL-7777

THIUM/CHALCOGEN SECONDARY CELLS FOR OMPONENTS IN ELECTRIC VEHICULAR-PROPULSION NERATING SYSTEMS

E. J. Cairns, E. C. Gay, M. L. Kyle,
A. D. Tevebaugh, L. E. Trevorrow,
W. J. Walsh, and D. S. Webster

ARGONNE NATIONAL LABORATORY, ARGONNE, ILLINOIS

Printed in the United States of America
Available from
National Technical Information Service
U.S. Department of Commerce
5285 Port Royal Road
Springfield, Virginia 22151
Price: Printed Copy $3.00; Microfiche $0.95

ANL-7777
Chemistry

ARGONNE NATIONAL LABORATORY
9700 South Cass Avenue
Argonne, Illinois 60439

LITHIUM/CHALCOGEN SECONDARY CELLS FOR COMPONENTS IN ELECTRIC VEHICULAR-PROPULSION GENERATING SYSTEMS

Interim Technical Summary Report No. 3
for May 23, 1970, to November 22, 1970

by

E. J. Cairns, E. C. Gay, M. L. Kyle,
A. D. Tevebaugh, L. E. Trevorrow,
W. J. Walsh, and D. S. Webster

Chemical Engineering Division

Prepared for
U. S. Army Mobility Equipment Research and Development Center
Fort Belvoir, Virginia

Project Order No. MERDC 175-69
Project/Task/Work Unit IT662705A012/02/042

March 1971

FOREWORD

This is Interim Technical Summary Report No. 3 of a research and development program conducted by the Chemical Engineering Division of Argonne National Laboratory under an agreement with the U.S. Army Mobility Equipment Research and Development Center, Fort Belvoir, Virginia. The project order number is MERDC A1048. The period covered by this report is May 23, 1970 through November 22, 1970.

The long-term goal of this program is to develop the technology for construction and testing of 50-kilowatt lithium/chalcogen secondary batteries for use in military vehicles. The immediate goals are the testing of single lithium/chalcogen cells (31.6-cm^2 active area), followed by the construction and testing of small (near 1 kW) batteries.

Overall program management is the responsibility of Dr. R. C. Vogel, Division Director, and Dr. A. D. Tevebaugh and Mr. D. S. Webster, Associate Division Directors. Technical direction is provided by Dr. E. J. Cairns, Section Head, Dr. W. J. Walsh, Group Leader, and Dr. E. C. Gay, Problem Leader. The contracting Officer's Technical Representative is Dr. J. R. Huff.

TABLE OF CONTENTS

LIST OF ILLUSTRATIONS

LIST OF ILLUSTRATIONS (Continued)

LIST OF TABLES

LITHIUM/CHALCOGEN SECONDARY CELLS FOR COMPONENTS IN ELECTRIC VEHICULAR-PROPULSION GENERATING SYSTEMS

Interim Technical Summary Report No. 3
for May 23, 1970, to November 22, 1970

by

E. J. Cairns, E. C. Gay, M. L. Kyle, A. D. Tevebaugh,
L. E. Trevorrow, W. J. Walsh, and D. S. Webster

ABSTRACT

The long-term goal of this program is to develop the technology for construction and testing of 50-kW lithium/chalcogen secondary batteries for the propulsion of electrically driven military vehicles. The immediate goals are the testing of single lithium/chalcogen cells followed by the testing of small (near 1 kW) batteries. Twenty-eight cells were tested during this reporting period. Tests of selenium-thallium and sulfur-thallium mixtures showed promise of achieving the required short-time peak power density of 1 to 3 W/cm^2 and showed no indications of cathode-material transport to the anode.

A procedure has been developed for fabrication of 7.5-cm diameter paste electrolytes by the molten salt infiltration of disks pressed from pure powdered lithium aluminate. The important property of disks made by this procedure is the low permeability to helium, less than 0.04 ml (STP) min^{-1} cm^{-2} atm^{-1} for 0.25-cm thickness. A number of disks of this type were fabricated for use in cell tests to determine whether the selenium transport rate was less than for previously tested pastes.

Chromium, aluminum, and beryllium were the most corrosion-resistant materials tested in the Li-Se alloys at 375°C in 600-hour tests.

SUMMARY

The battery program for hybrid electric vehicle propulsion, U.S. Army (Fort Belvoir), has as its ultimate goal the development of high-specific-power, multikilowatt, lithium/chalcogen secondary batteries to provide acceleration and hill-climbing power for electrically driven Army vehicles. The present, shorter-term objective is to develop 7.5-cm diameter cells with paste electrolytes capable of 1 to 3 W/cm^2 short-time peak power densities which have lifetimes of 1000 to 2000 hr and 1000 to 2000 charge-discharge cycles. Earlier investigations[1] of lithium/selenium cells resulted in an energy density of 0.5 W-hr/cm^2

at the 1-hour discharge rate (0.27 A/cm^2), the capability of delivering 52% of the theoretical capacity density at this rate, a short peak power density of 2.3 W/cm^2, and an ampere-hour efficiency of 0.92. Efforts devoted to the development of sealed lithium/selenium cells with 100-hr life (the immediate goal of the program) at this high performance were unsuccessful because of selenium transport through the paste electrolyte to the lithium anode, resulting in a gradual loss of performance with time.

Investigations of various techniques to eliminate this selenium transport resulted in a promising approach to the solution of the problem, namely, the addition of various elements to the selenium in order to decrease the transport rate and the solubility of selenium-bearing species in the electrolyte. Tests of selenium-thallium and sulfur-thallium mixtures as cathode materials show promise of achieving the required short-time peak power density of 1 to 3 W/cm^2 and show no indications of cathode-material transfer to the lithium anode. Sulfur-thallium mixtures are of interest because of the lower equivalent weight of sulfur compared with selenium. Present efforts are directed toward determining the capacity and life of cells using selenium-thallium and sulfur-thallium cathodes.

A procedure has been developed for fabrication of 7.5-cm diameter paste electrolytes by the molten salt infiltration of disks pressed from pure powdered lithium aluminate. The important property of disks made by this procedure is their low permeability to gaseous helium, less than 0.04 ml (STP) min^{-1} cm^{-2} atm^{-1} for 0.25-cm thickness. A number of disks of this type were fabricated for use in cell tests to determine whether the selenium transport rate was lower than for previously tested pastes.

High-temperature polymers were considered as possible lightweight hermetic sealants and electrical insulators for Li/Se cells. None of the twenty-one polymers tested demonstrated the required corrosion resistance under cell conditions. Attempts to provide hermetically sealed cells will now be directed primarily toward metal-ceramic seals and other high-temperature sealants.

The corrosion resistance of a number of materials to Li-Se alloys was tested to determine their suitability for cathode containment. Chromium, aluminum, and beryllium were the most corrosion-resistant materials tested in the Li-Se alloys at 375°C in 600-hr tests. Chromium has consistently performed well with corrosion rates less than 0.15 mm/yr (6 mpy). Aluminum has exhibited corrosion rates from 0.01 to 0.4 mm/yr and beryllium has shown rates from 0.01 to more than 1.8 mm/yr.

INTRODUCTION

The secondary lithium/chalcogen batteries being developed at Argonne National Laboratory have projected capabilities appropriate for hybrid electric vehicular propulsion. The batteries, which will operate at temperatures in the range of 250 to 460°C, will be composed of cells with liquid lithium anodes, immobilized fused-salt electrolytes (in the form of a rigid paste), and liquid chalcogen cathodes containing various chemical additives. The performance goals of the present laboratory cells, with 7.5-cm diameter paste electrolytes, are 1 to 3 W/cm^2 short-time peak power density and a specific energy of 170 W-hr/kg (at the 1-hr rate*); these goals have been achieved with lithium/selenium cells for short periods of time.[1] The cells currently being tested, containing selenium or sulfur and various chemical additives as the cathode, are expected to satisfy both the performance and lifetime requirements needed for use in hybrid electrically driven vehicles.

During this reporting period, Li/Se, Li/Se-As, Li/Se-P, Li/Se-Tl, Li/Se-Te, Li/P_4S_{10}, and Li/S-Tl cells were tested to identify the cathode compositions which will satisfy the cell performance and lifetime requirements of this program. The primary electrode reactions during discharge in these cells are as follows:

$$\text{Anode:} \quad xLi \rightarrow xLi^+ + xe^- \tag{1}$$

$$\text{Selenium Cathode:} \quad xLi^+ + ySe + xe^- \rightarrow Li_xSe_y \tag{2}$$

$$\text{Sulfur Cathode:} \quad xLi^+ + mS + xe^- \rightarrow Li_xS_m \tag{3}$$

The highest lithium-to-selenium and lithium-to-sulfur ratios achieved in the cathode during cell discharge correspond to the stable compounds Li_2Se and Li_2S, respectively. These stoichiometric values are the basis for the calculation of theoretical capacity densities reported below. The capacity attributed to the various elements added to the selenium and sulfur was calculated assuming two equivalents/mole (e.g., assuming Li_2Te and Li_2P_5 as the final discharged products). In cells containing the thallium alloys (Tl_2Se_3 and TlS_2), it is believed that the products of the cell reactions are Li_2Se, Li_2S, and higher thallium content alloys. Chemical analyses of the various products will be made to determine more accurately the theoretical capacity for those cathode mixtures of major interest.

---

*The 1-hr rate, 0.26 A/cm^2, was determined from performance measurements of Li/Se cells and is the current density at which the voltage of a fully-charged cell will reach 1.0 V in 1 hr. The 1.0 V cut-off is arbitrary; cells may be discharged to zero volts if desired. Measurements will be made to determine the capacity of these cells below 1.0 V.

Reactions 1, 2, and 3 are reversible and can take place at very high rates with very little decrease in cell voltage. The exchange-current densities are in the range of several amperes per square centimeter.[2] Because of this, the only significant voltage losses in a lithium/chalcogen cell are those due to the internal resistance of the cell (resistance overvoltage) and slow mass transport in the chalcogen electrode (diffusion overvoltage).

The effort for development of these cells is concentrated in the following areas:

Task 1. Lithium/Chalcogen Cell Studies for Electric Vehicle Propulsion

- A. Lithium/Chalcogen Cell Electrical Performance Studies
- B. Life-Testing and Charge-Discharge Cycle Testing of Lithium/Chalcogen Cells
- C. Design of High-Specific-Power Lithium/Chalcogen Cells
- D. Automatic Charge-Discharge Testing of Multiple Lithium/Chalcogen Cells

Task 2. Studies of Paste Electrolytes for Lithium/Chalcogen Cells

Task 3. Studies of Sealants and Insulators for Lithium/Chalcogen Cells

Task 4. Studies of Corrosion by Lithium/Chalcogen Mixtures

Task 5. Lithium/Chalcogen Battery Studies

Task 1, involving cell studies, has as its objective the development of 7.5-cm diameter cells (31.6-cm^2 active area) having 1 to 3 W/cm^2 short-time peak power density and having a long life (1000 to 2000 hr and 1000 to 2000 cycles). In order to achieve this objective, the current density-voltage and voltage-time behavior of the cells are measured, cell design changes are made as required to improve the electrical performance, and various elements are added to the selenium or sulfur cathode materials to prevent transfer of these chemicals to the anode and the resulting short cell life observed with pure selenium cathodes. Short-range objectives are (1) to maintain a peak power density of 1.5 to 2 W/cm^2 for 3 seconds and an average power density of 1.0 W/cm^2 for 15 minutes, (2) to develop cells with a charge-discharge energy efficiency of at least 50% to 1.0 V at the 1-hr rate and a coulombic efficiency of 95%, (3) to

optimize the cathode current collector configuration to increase the percentage of theoretical capacity achieved to 40-50% at the 1-hr rate and (4) to develop cells with a life of 100 hr during cycling at the 1-hr rate (to a 1.0 V cut-off).

Problems were experienced in Task 1 with maintaining high performance of Li/Se cells over long periods of time (100 hr and longer). The limiting factor appeared to be the formation of Li_2Se at the lithium-paste electrolyte interface, resulting in a considerable increase in the cell resistance and a decrease in the cell capacity. A portion of the selenium transferred to the anode appeared to have migrated through pores and/or microcracks in the paste electrolyte. Recent test results (results obtained with improved pastes which reduced or eliminated selenium transfer through pores or cracks) indicated that a portion of the cathode-material transfer to the anode may be associated with the solubility in the electrolyte of selenium-rich phases formed in the cells during discharge. The most recent solubility results indicate that there is a possibility of higher selenium solubility in the electrolyte than previously estimated. These solubility results and investigations of the pseudo-ternary system Li_2Se, Se, and lithium halide eutectic are discussed to provide background information to indicate the need for using selenium alloys in later cell investigations in an attempt to minimize the cathode material solubility in the electrolyte.

Previously reported values[3] for the solubility of selenium in molten LiF-LiCl-LiI indicated that very little selenium (< 0.1 mol %) dissolves in molten lithium halides in the 350-500°C range. A more recent study* was conducted to determine the effect of the presence of Li_2Se on the solubility of selenium in molten lithium halides. Saturated solutions were prepared of Li_2Se, selenium, and an Li_2Se-selenium mixture (Se/Li_2Se mole ratio = 4.0) in the LiBr-RbBr eutectic at 365 ± 1°C. After each solute was equilibrated with the salt, a portion was filtered and analyzed for selenium content. A substantial increase was noted in the solubility of selenium from the Li_2Se-Se mixture (1.5 mol %) when compared with the cases where Li_2Se alone (0.03 mol %) and selenium alone (0.03 mol %) were the solutes. This may be due to the formation of soluble polyselenides, Se_x^{-n}, where the values of x and n remain to be determined.

An investigation of the pseudo-ternary system Li_2Se, Se, LiX (where LiX is the LiBr-RbBr or LiF-LiCl-LiI eutectics) was undertaken to resolve apparent discrepancies between the lithium-selenium phase diagram and results of emf studies.[3] The original assumption for the emf cell was

*V. A. Maroni, private communication, 1970.

that the cathode could be considered to be a simple binary lithium-selenium mixture. The emf studies gave results indicating a wide range of immiscibility, i.e., emf constant with changing composition at fixed temperatures, but the boundaries of immiscibility were inconsistent with results from the phase diagram for lithium selenide-selenium. At this point, the solubility results discussed above were available (indicating that selenium solubility in molten electrolytes was enhanced by the presence of Li_2Se) and caused a reevaluation of the role of the electrolyte in the emf cell.

Before considering further the pseudo-ternary system, a review is given below of what is known or presumed concerning the binary and pseudo-binary systems involved. The lithium selenide-selenium binary system has been well studied and is essentially as presented in the literature[3] and shown in the lithium-selenium phase diagram, Fig. 1. Starting from the Li_2Se phase, the upper liquidus decreases sharply with the lithium-rich liquid, L_2, undergoing monotectic reaction at 350°C to form a selenium-rich liquid, L_1, and Li_2Se. The monotectic composition is about 22 mol % Li_2Se. The miscibility region between L_1 and L_2 extends from below 0.4 mol % Li_2Se to 22 mol % Li_2Se. Liquid L_1 freezes at 220°C, the freezing point of pure selenium. Less is known about the selenium-alkali halide systems. Presumably they have no intermediate phases, although rubidium-selenium compounds may present complications for the Se-(LiBr-RbBr) system. Solubility studies indicate that the mutual solubilities in these systems are quite low*. Thermal analyses indicate that the presence of selenium does not alter the melting point of the alkali halide eutectics and vice versa**.

On the basis of the data obtained from emf studies and from what is known about the binary systems, the pseudo-ternary isothermal sections shown in Figs. 2 and 3 were proposed***. The two liquid phases present in the lithium selenide-selenium binary are seen to extend into the ternary phase diagram at the temperatures of these sections, and the designations L_1 and L_2 are retained. The alkali halide-rich liquid, L_3, also extends into the ternary diagram. There appears to exist a three-liquid equilibrium, $L_1 + L_2 + L_3$, which is undesirable. Selenium alloyed with additives such as thallium is being investigated in an attempt to eliminate or reduce this region of mutual solubility.

The major objective of Task 2, paste-electrolyte studies, was to devise methods for eliminating the permeability of the paste electrolyte

---

* V. A. Maroni, private communication, 1970.

** P. Cunningham, private communication, 1970.

*** E. J. Cairns, G. H. Kucera and P. T. Cunningham, presented at the CITCE Meeting, Prague, Sept. 1970.

Fig. 1. Phase Diagram of the Lithium-Selenium System.

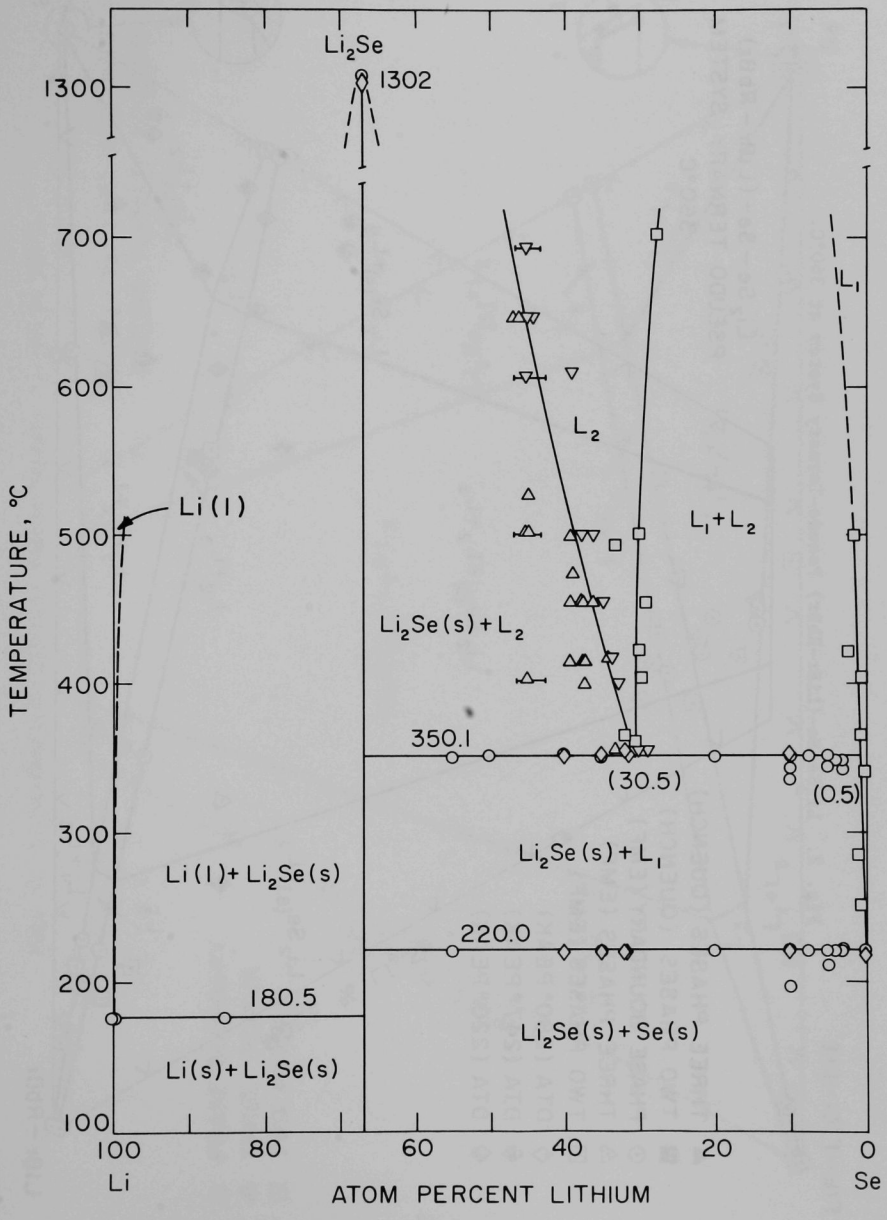

Fig. 2. Li_2Se-Se-(LiBr-RbBr) Pseudo-Ternary System at 360°C.

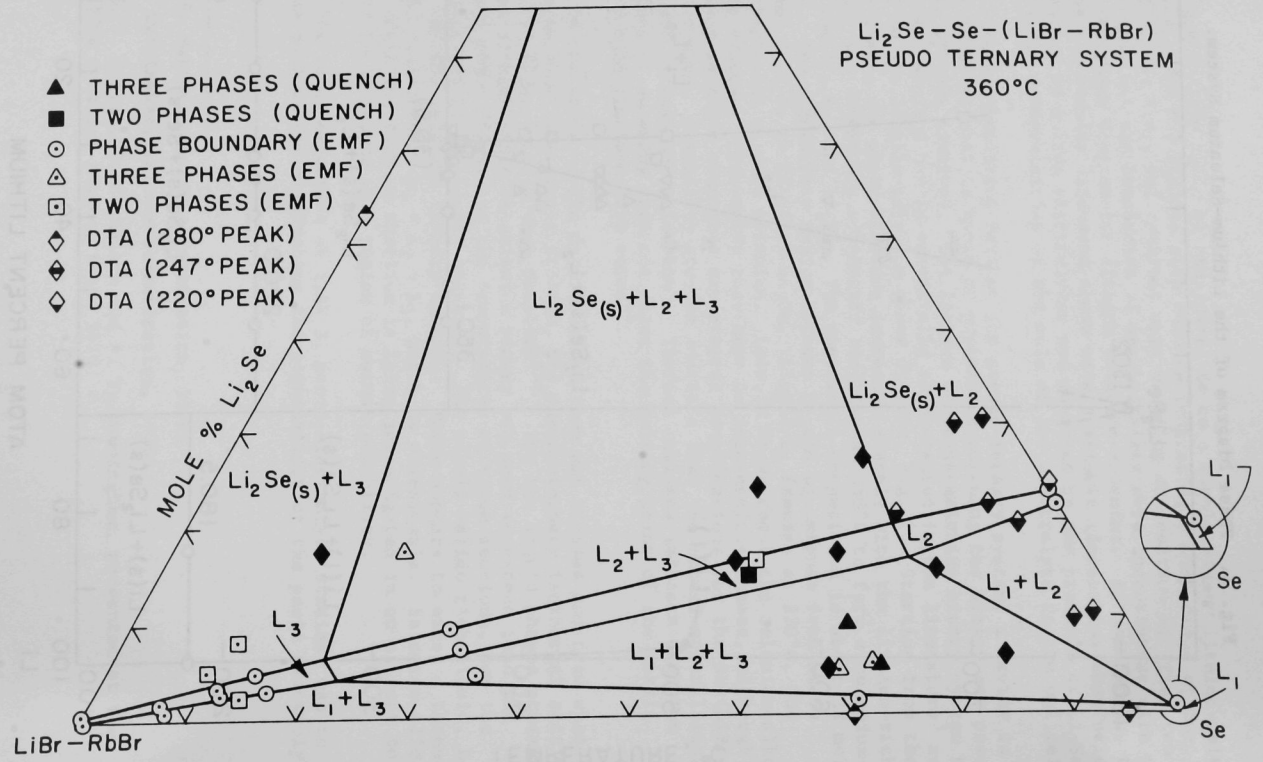

Fig. 3. Li_2Se-Se-(LiF-LiCl-LiI) Pseudo-Ternary System at 390°C.

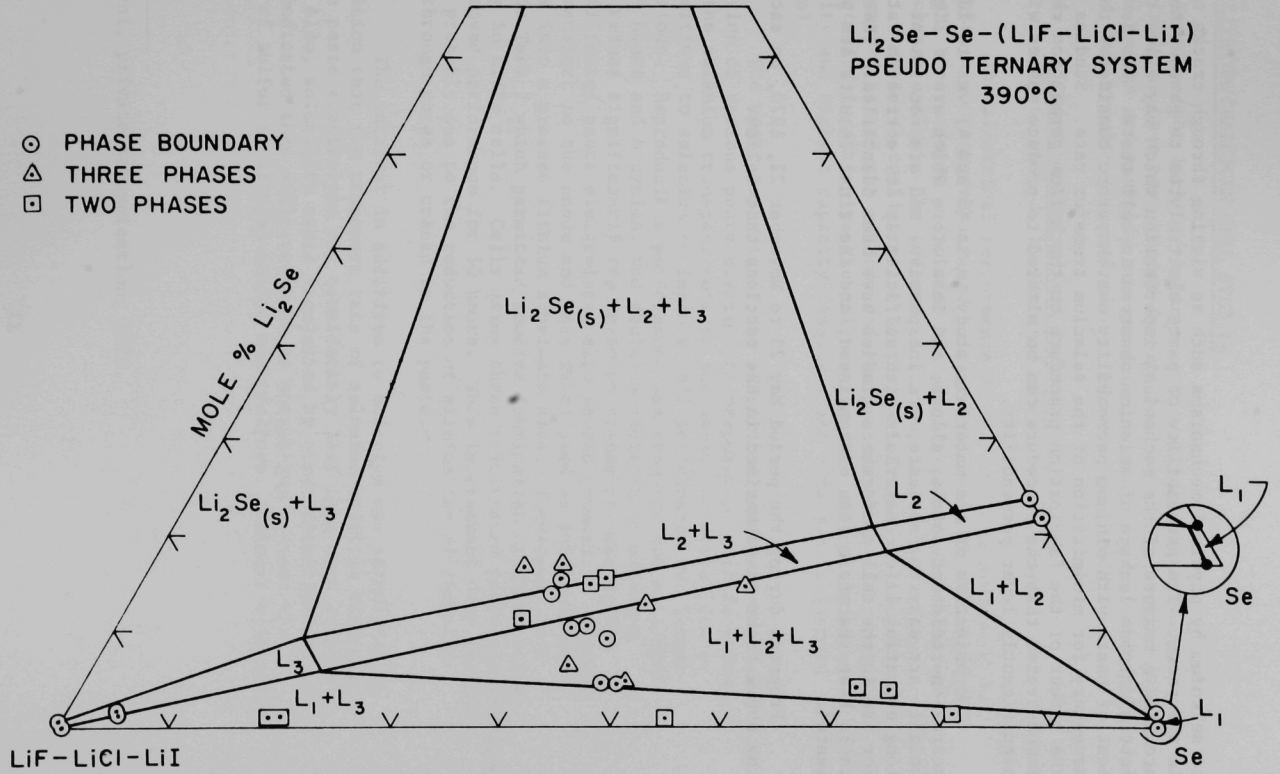

to selenium by physical mechanisms such as wicking through cracks or pores in the paste. The permeability of paste electrolytes to gaseous helium provided a measure of the mechanical imperfection which may allow the interelectrode leakage of selenium observed in cell tests. The development of paste with minimum permeability was therefore considered to be necessary for minimization of the selenium transfer rate. Studies of the effect of the fabrication procedure on the helium permeation rate demonstrated that the procedure can be altered to produce pastes with significantly lower permeability.

The objective of the materials study tasks (3 and 4) was to identify corrosion-resistant metals, alloys, and insulators which are of light weight, are easy to fabricate, are inexpensive, and are consistent with long operating life. Materials with sufficiently low corrosion rates for use in the cell performance studies have been identified. These tasks have therefore been discontinued, and the final results are presented.

Progress during the period May 23 to November 22, 1970, on each of the above tasks is summarized in the sections that follow.

TASK 1. LITHIUM/CHALCOGEN CELL STUDIES

Twenty-eight lithium/chalcogen cells with 7.5-cm diameter paste electrolytes have been tested during this reporting period. Details of the cell design and assembly are given below, followed by discussions of selected test results for several of the individual cells.

A. Lithium/Chalcogen Cell Performance Studies

(E. C. Gay, J. E. Kincinas, and J. D. Arntzen)

The electrical performance of the cells is evaluated in terms of voltage-current density and voltage-time behavior during constant-current discharge as a function of cell structure and number of charge-discharge cycles. The effects of various paste electrolyte treatments, structural configuration of the cathode current collector, chemical composition of the cathode and changes of other cell parameters are being studied to determine the cell design that yields the highest power density and highest capacity density (with efficient chalcogen utilization).

The major emphasis of the electrical performance studies was evaluation of various paste electrolyte preparation methods intended to reduce the selenium transport rate to the anode and evaluation of various additives to selenium to improve cell performance for longer testing periods. Reproducible performance was measured for a Li/Se-P cell for 56 hours and 6 cycles, and thallium addition to selenium appears to reduce significantly the selenium transport rate to the anode. Infiltrated paste electrolytes also showed promise of reducing selenium transport to the anode and were fabricated by infiltrating electrolyte into a pressed lithium aluminate disk. Techniques were developed in Task 2 which permitted routine fabrication of these disks for testing in Li/Se cells. Cells using these infiltrated paste electrolytes showed improved performance for 50 hours. This improvement over earlier results is probably due to the reduction or elimination of selenium transport through pores or cracks in the paste.

The interest in additives to selenium was stimulated by the recognition that the transport rate of selenium-additive mixtures through the paste electrolyte was considerably less than that of pure selenium. Also, solubility tests (conducted by other investigators at Argonne*) indicated that additives such as phosphorus reduced the solubility of sulfur in lithium-halide electrolytes. Reduced solubility

---

*V. A. Maroni, private communication, 1970.

of the cathode material in the electrolyte is of particular significance in developing cells capable of long life. The procedure for selecting additives to selenium consisted of (1) examination of available phase diagram data for lithium-additive and selenium-additive systems to identify those systems with low melting points over reasonable composition ranges (an apparent requirement for high utilization of the theoretical capacity), (2) a brief evaluation of the additive effect on selenium solubility in the electrolyte (future plans might include solubility measurements on the most promising mixtures), and (3) an evaluation of the additive effect on cathode conductivity in terms of obtaining 1 to 2 W/cm^2 peak power density.

The disadvantages of the addition of elements to selenium are the reduction of cell capacity density and the possibility of increased cell weight, such as in the case of thallium-selenium alloys. These disadvantages may be circumvented, however, by adopting one or more of the following approaches: redesigning the cell (i.e., by using viscous-electrolyte cells, which have lower electrical resistance than do paste-electrolyte cells), using the minimum additive composition which reduces the cathode-material transport to the anode, and using lower density alloys (such as thallium-sulfur).

(1) Cell Components

The cell configuration was described in detail in Report No. 2[1] and was shown in Fig. 1, p. 7, of that report. A modification in the cathode current collector was made for some of the cells and is discussed in appropriate sections below. The cell components consisted of (a) a boron nitride ring, which insulated the anode from the cathode compartment and served as part of the anode housing, (b) a stainless steel Feltmetal anode (Huyck Metal Co.; 302 SS, 1.6 mm or 3.2 mm thick, 90% porosity, 67-μm mean pore size) that had been soaked in lithium at 550°C, (c) a Nb-1% Zr cathode cup containing niobium expanded mesh of approximately 63% or 90% porosity (0.23-cm die size) or containing niobium ribs (to provide support for the paste electrolyte without restricting cathode-material convection), (d) voltage and current leads welded to the cell clamping plate and the anode cup (this plate was insulated from the anode by an alumina disk), and (e) Inconel-X springs, which provided good electrical contact for the anode and cathode current collectors with the paste electrolyte and also provided peripheral sealing force to the paste electrolyte-grooved cathode housing sealing surface. A Grafoil* gasket (compressed graphite material) was used at the paste electrolyte/cathode sealing surface to prevent cathode leakage in cells containing sulfur mixtures.

*A product of Union Carbide Corporation.

The paste electrolytes were prepared using lithium aluminate and/or boron nitride filler (of approximately 46-m^2/g and 7-m^2/g specific surface area, respectively) and LiF-LiCl-LiI, LiBr-RbBr, or LiCl-LiBr-LiI-KI-CsI eutectics. These eutectics have compositions (in mole percent) of 11.7% LiF - 29.1% LiCl - 59.2% LiI, 59% LiBr - 41% RbBr, and 3.7% LiCl - 9.1% LiBr - 52.3% LiI - 15.7% KI - 19.2% CsI. The melting points of these eutectics are approximately 340.9°C, 259°C, and 184°C, respectively.

A description of the paste electrolytes and quantities of lithium and cathode material loaded into the various cells are given in Table 1. The various cathode mixtures shown in this table were prepared by (1) loading the weighed ingredients into a quartz capsule, (2) evacuating and sealing the capsule, (3) heating the mixture to 500°C for several hours, and (4) cooling the mixture rapidly, removing the product from the capsule, and loading it into the cathode cup. The cathode compositions used in the additive investigation are given in Table 2.

(2) Experimental Procedures for Electrical Performance Testing

The components of the 7.5-cm diameter paste electrolyte cells were assembled in a helium atmosphere glovebox of less than 1 ppm moisture, nitrogen and oxygen content. The assembled cells were mounted in a stainless steel furnace well containing an alumina crucible for electrical insulation from the well. The furnace well was sealed in the glovebox with a SS cover provided with electrically insulating fittings for the current and voltage leads and thermocouple well. The sealed furnace well was transferred from the glovebox to a testing station in a vacuum-frame hood. The testing equipment consisted of (1) a tube-type electric resistance furnace mounted in the horizontal position, (2) flexible helium-gas, electrical and vacuum leads, (3) a temperature recorder and controller, (4) a two-pen recorder for cell voltage and current measurements, and (5) a 40-V, 200-A dc power supply.

The cells were charged and discharged at constant currents with the aid of the high-current dc power supply. Usually, discharge data were taken from the fully charged condition (open-circuit voltage of 2.2 V for the Li/Se cell), and charge data were taken from the partially discharged condition. The cell resistance was calculated from short-time (a few seconds after closing the circuit) cell voltage and current-density measurements made with a two-pen recorder having a 1/4-second response. These measurements were made so rapidly that there was a negligible overvoltage (< 0.02 V) due to mass transport of reactants to or removal of products from the paste electrolyte-cathode interface.

Table 1. Lithium/Chalcogen Cells with 7.5-cm Diameter Paste Electrolytes

Cell No.	Theor. Capacity[a] (A-hr)	Anode Lithium Content (g)	Cathode Material Weight (g)	Paste Electrolyte: Electrolyte Content (wt %) LiF-LiCl-LiI	LiBr-RbBr	LiCl-LiBr-LiI-KI-CsI	$LiAlO_2$ Filler (wt %)	Fraction of Theor. Density	Thickness (cm)	Cathode Composition (wt %)
23	11.9	5.2	21.8	57.0			21.5[b]	0.96	0.25	11.9 Se-58.7 Li_2Se-29.4 Te
24	20.4	5.0	20.4		60.0		40.0	0.97	0.25	56.7 Se-43.3 Te
25	20.0	4.0	29.4			44.5[c]	44.5	0.87	0.28	100 Se
26	10.6	5.6	28.9		60.0		40.0	0.95	0.25	100 Se
27	17.7	5.2	26.0			41.4[d]	41.4	0.83	0.29	100 Se
28	19.2	5.8	28.2	60.0			40.0	0.95	0.26	100 Se
29	18.0	4.8	10.0			50.0	50.0	0.85	0.28	100 P_4S_{10}
L-4[e]	20.2	5.2	40.9	57.0			21.5[b]	0.96	0.25	30 Se-70 Te
LW-1[e]	16.4	8.5	24.1		60.0		40.0	0.97	0.25	100 Se
L-6[e]	22.7	5.0	33.4	56.2[f]			43.8	0.88	0.28	100 Se
30	12.7	5.9	26.5	60.0			40.0	0.90	0.26	55.7 Se-11.9 As-32.4 LiCl-LiBr-LiI-KI-CsI
31	10.5	5.0	29.7			50.0	50.0	0.83	0.28	52.2 Se-8.0 P-39.8 LiCl-LiBr-LiI-KI-CsI
32	15.7	3.7	20.3	58.5			41.5	0.90	0.25	78.8 Se-21.2 LiF-LiCl-LiI
33	22.3	4.2	32.8	60.0[f]			40.0	0.98	0.28	100 Se

Footnotes on p. 16

Table 1, (continued)

Cell No.	Theor. Capacity (A-hr)	Anode Lithium Content (g)	Cathode Material Weight (g)	Paste Electrolyte: Electrolyte Content (wt %) LiF-LiCl-LiI	LiBr-RbBr	LiCl-LiBr-LiI-KI-CsI	$LiAlO_2$ Filler (wt %)	Fraction of Theor. Density	Thickness (cm)	Cathode Composition (wt %)
34	14.1	9.1	23.6	60.0			40.0	0.94	0.26	87.7 Se-8.9 P-3.4 Li_2Se
35	12.3	5.3	18.1	60.0			40.0	0.92	0.26	100 Se
36	26.0	5.2	20.0		60.0		40.0	0.96	0.25	100 P_4S_{10}
38[g]	29.6	5.5	22.8		70.0		30.0	0.95	0.22	100 P_4S_{10}
39	20.8	4.3	30.6	55.4[h]			44.6	0.88	0.28	100 Se
40	20.5	8.3	30.1	57.2[h]			42.8	0.89	0.28	100 Se
41	34.8	4.1	51.2		70.0		30.0	0.98	0.25	100 Se
42	19.3	4.9	28.4	56.2[h]	70.0		30.0 43.8	0.98 0.88	0.24 0.28	100 Se
43	20.6[k]	5.4	82.6		73.0[i]		27.0	0.96	0.27	36.6 Se-63.4 Tl
44	19.9	6.5	29.3	60.0[f]			40.0	0.90	0.30	100 Se
45	26.8[l]	4.0	67.0	56.8			43.2	0.88	0.28	23.9 S-76.1 Tl
46	21.0[k]	3.9	84.2			60.0	40.0	0.93	0.24	36.6 Se-63.4 Tl
47	24.4[l]	5.5	60.9	64.5			22.1[j]	0.91	0.26	23.9 S-76.1 Tl
48	26.8[l]	4.1	67.0	56.8			43.2	0.88	0.27	23.9 S-76.1 Tl

Footnotes on next page.

FOOTNOTES

[a] This theoretical capacity was calculated based upon two equivalents/mole for the quantity of loaded cathode material (i.e., assuming that the fully discharged products are Li_2Se, Li_2S, Li_2Te, etc.).

[b] The paste electrolyte filler consisted of 21.5 wt % BN and 21.5 wt % $LiAlO_2$.

[c] This cell contained 4.7 g electrolyte (11 wt % of the paste) in the cathode.

[d] This cell contained 8 g electrolyte (17.2 wt % of the paste) in the cathode.

[e] Cell numbers containing the letter "L" were tested by V. M. Kolba.

[f] A totally infiltrated disk was used in this cell (infiltrating the electrolyte into a pressed $LiAlO_2$ filler disk).

[g] An attempt was made to infiltrate a paste electrolyte under vacuum for Cell No. 37, but the paste cracked prior to testing.

[h] A modified infiltrated paste electrolyte was used for this cell (salt-poor filler was pressed into the shape of a disk and additional salt was infiltrated after pressing).

[i] The conventional LiBr-RbBr paste was coated with 9.4 wt % LiF-LiCl-LiI eutectic to improve lithium wetting.

[j] The paste electrolyte for Cell No. 47 contained 22.1 wt % $LiAlO_2$ and 13.4 wt % BN filler.

[k] This theoretical capacity was calculated based on the selenium content of the cathode.

[l] This theoretical capacity was calculated based on the sulfur content of the cathode.

Table 2. Cathode Compositions Tested in the Additive Investigation

Cell No.	Cathode Composition (wt %)								
	Se	S	P_4S_{10}	P	As	Te	Tl	Li_2Se	Salt Additiv
23	11.9					29.4		58.7	
24	56.7					43.3			
29			100.0						
L-4	30.0					70.0			
30	55.9				11.7				32.4
31	52.2			8.0					39.8
34	87.7			8.9				3.4	
36			100.0						
38			100.0						
43	36.6						63.4		
45		23.9					76.1		
48		23.9					76.1		

[a]The LiCl-LiBr-LiI-KI-CsI eutectic.

Another portion of the cell performance testing included measurement of cell voltage as a function of time during constant-current discharge. These curves were used to calculate the voltage vs capacity density curves, which are presented with resistance and diffusion overvoltages included and also with only diffusion overvoltage included. The voltage difference between these curves is the resistance overvoltage. These curves are termed "IR-included" and "IR-free," respectively. The resistance overvoltage is the sum of the overvoltages caused by the electronic resistance of the cell parts, the accumulated cell reaction products at the cathode-electrolyte interface, the contact resistance associated with insufficient wetting of the paste electrolyte by the electrode materials, the electrolytic resistance of the paste electrolyte, and the resistance of corrosion products formed on some current collector materials.

The theoretical capacity was calculated based upon two equivalents/mole for the quantity of loaded cathode material (i.e., assuming that the fully discharged products are Li_2Se, Li_2S, Li_2Te, etc). The current-density and capacity-density values were based on the active paste electrolyte area of 31.6 cm^2 unless specified otherwise.

(3) Electrical Performance

Earlier experimental results from Li/Se cell tests indicated that cell life was limited by selenium transport to the anode. Helium permeability measurements suggested that a portion of the selenium transport occurred through pores or microcracks in the paste. This and other undetermined transport mechanisms appeared to be suppressed best by the use of totally infiltrated paste electrolytes and the addition of various elements to selenium. A major objective of the electrical performance studies therefore was evaluation of different paste-electrolyte fabrication techniques for reducing selenium transport to the anode through pores and microcracks in the paste. Another area of investigation was the evaluation of various elements added to selenium to reduce selenium transport rate to the anode. The objective of these tests was to achieve satisfactory cell performance for a period of 100 hr or longer. The procedure for selecting selenium additives was discussed earlier in this report [Task 1, Section A(1)]. The goal of this study was to find a selenium additive or other cathode material, such as sulfur, which (1) eliminates cathode-material transport through the paste, and (2) causes a minimum decrease from the performance measured for lithium/selenium cells.

Since permeability of paste electrolytes to gaseous helium implies the existence of mechanical imperfections as a possible cause of the interelectrode leakage of selenium observed in cell tests, the development of a capability for fabricating pastes with minimum permeability was considered to be a basic requirement. Studies of the

effect of fabrication procedure on permeability (investigation conducted in Task 2) demonstrated that these procedures can be altered to produce pastes with significantly lower leak rates. The helium permeability of several paste electrolytes subsequently used in cell tests is shown in Table 3. The results of cell tests using these paste electrolytes are shown in Table 4. From these results, it was observed that the totally infiltrated pastes showed significantly lower selenium permeability for open circuit testing (under conditions of no charge and discharge measurements), but the selenium transport rate increased with performance testing (10 wt % and 38 wt % Se transferred, respectively). Also, the selenium transport rate at 300°C with performance testing was extremely low compared with the transport rate at the normal operating temperature of 380°C. This low selenium transport at 300°C was observed for the conventional pastes, which normally showed a much higher helium permeability than infiltrated pastes. The conventional paste electrolytes also showed low transport of such cathode materials as P_4S_{10}. These results suggested that the addition of various elements to selenium and lower operating temperature may change the physical and/or chemical properties of selenium to a degree sufficient to drastically reduce the transfer rate of selenium to the anode. These experimental results are inconclusive, however, as to the fraction of the selenium transported through the paste by each mechanism. Since the totally-infiltrated paste showed a major reduction in the helium permeability and yet showed inadequate reduction in selenium transfer rate, the addition of various elements to selenium appeared to be the best approach to reduce the rate of selenium transfer. Based on the reduced helium permeability, it was believed that the infiltrated paste electrolyte significantly reduced selenium transport through pores or microcracks in the paste. Since performance measurements with these pastes indicated that there was still a significant selenium transport rate (the transport rate was significantly less, however, than measured for conventional paste electrolytes), the implication was that some other selenium transport mechanism (possibly selenium solubility in the electrolyte) was important. Results from preliminary tests with additives to selenium showed the largest reduction in selenium transport rates. Therefore, our efforts are presently being concentrated in the area of addition of various elements to selenium or sulfur to minimize the cathode-material transfer rate. A detailed description of several of the paste electrolyte tests shown in Table 4 is presented below in Sections (a) to (d).

Table 2 shows the various cathode compositions tested in the additive investigation. Table 5 summarizes the results of these tests. Phosphorus, tellurium and thallium were found to be effective additives to selenium and sulfur for reducing the cathode material transfer rate. Tellurium and thallium showed the most promise of meeting the short-time peak power density requirement of 1 to 3 W/cm^2. Thallium, however, appears more attractive than tellurium because of its much lower corrosion rates in cell tests using niobium current collectors.

Table 3. Helium Permeability of 7.5-cm Diameter Paste Electrolyte

Cell Number	Disk Number	Paste Electrolyte: Electrolyte Content (wt %)[a] LiF-LiCl-LiI	LiBr-RbBr	LiCl-LiBr-LiI-KI-CsI	Fraction of Theoretical Density	Fabrication Method[b]	Permeability [ml He(STP) $min^{-1}cm^{-2}$ at 1 atm differential and 25°C]
28	49	60			0.95	conventional	0.93
29	47			50.0	0.85	conventional	1.11
L-6	2202F32	56.2			0.88	infiltrated	0.10
39	2202F48	55.4			0.88	salt-poor infil.	3.0
40	2202F51	57.2			0.89	salt-poor infil.	0.09
41	62A		70.0		0.98	conventional	1.2
42	2202F32M[c]	56.2			0.88	salt-poor infil.	0.1
44	2202F61	60.0			0.90	infiltrated	< 0.04

[a] Lithium aluminate was the filler material for all of the paste electrolytes.

[b] Conventional paste electrolytes were prepared by pressing a homogeneous electrolyte filler mixture. Salt-poor infiltrated pastes were prepared by pressing an electrolyte filler mixture of low electrolyte content with subsequent infiltration of additional electrolyte into the fabricated disk. Infiltrated pastes were prepared by pressing a pure filler disk and infiltrating all of the electrolyte into this disk.

[c] Disk 2202F32M and a conventional paste electrolyte were used in this cell.

Table 4. Selenium Permeability of 7.5-cm Diameter Paste Electrolyte

Cell Number	Disk Number	Paste Electrolyte Fabrication Method	Purpose of Experiment[a]	Results
29	47	conventional	Test P_4S_{10} permeability of LiCl-LiBr-LiI-KI-CsI paste electrolyte under conditions of no electrical performance measurements.	No product formation at anode; some P_4S_{10} lost (20 wt %) at seal.
L-6	2202F32	infiltrated	Test Se permeability of LiF-LiCl LiI infiltrated paste electrolyte under conditions of no electrical performance measurements.	10 wt % Se loaded in cathode transferred through paste forming Li_2Se at anode; permeability was 4 times lower for infiltrated pastes than for conventional pastes.
39	2202F48	salt-poor infil.	Test Se permeability of salt-poor infiltrated paste electrolyte with electrical performance measurements. This modified paste fabrication technique was required due to frequent cracking of paste electrolytes during attempts to infiltrate pure filler disks.	50 wt % Se loaded in cathode transferred through paste forming Li_2Se at anode; salt-poor paste showed more reproducible performance for 8 hr period than did conventional paste.
40	2202F51	salt-poor infil.	Same as for Cell No. 39.	Same as for Cell No. 39.
41	62A	conventional	Test a conventional paste (highest Se permeability at 380°C) at lower temp. (300°C) such that Li_2Se formed may exist as solid in liquid Se phase (selenium-rich liquid phase exists at 380°C).	No Li_2Se at anode; observations differed greatly from 40 to 50 wt % loaded Se normally found at paste/anode interface; poor performance at this operating temp.; some unidentifiable paper-thin layer found at anode.

[a]The testing period, with the exception of Cells No. 42 and 44, was approximately 45 hr. The temperature was 380°C except for Cell No. 41.

Table 4, (continued)

Cell Number	Disk Number	Paste Electrolyte Fabrication Method	Purpose of Experiment[b]	Results[a]
42	2202F32M	salt-poor infil. and conventional	Determine if diffusion resistance for Se or some Se-bearing species could be increased sufficiently for significantly improved performance. Attempted to increase diffusion resistance by doubling interelectrode distance (i.e., used 2 paste electrolytes).	Best performance achieved to date for selenium cathode over 4 cycles during first day of testing; after 56 hr testing, 40 wt % loaded Se transferred to the anode; reduced performance after 24 hr.
44	2202F61	infiltrated	Test Se permeability of LiF-LiCl-LiI infiltrated paste electrolyte under conditions of electrical performance measurements.	Reproducible performance for 50 hr; 38 wt % Se transferred to anode after 70 hr; higher Se transfer rate than observed for non-electrical test.

[a]The testing period, with the exception of Cells No. 42 and 44, was approximately 45 hours.

[b]Temperature was 380°C except for Cell No. 41.

Table 5. Electrical Performance of 31.6-cm^2 Lithium/Chalcogen-Additive Cells

Cell No.	Peak Power Density (W/cm^2)	Discharge Current Density (A/cm^2)	Average Discharge Voltage (V)	Discharge Time (hr)	Capacity Density ($A\text{-}hr/cm^2$)	Energy Density ($W\text{-}hr/cm^2$)	Fraction of Theoretical Capacity[a]	Fraction of 1-hr Rate Current Density[b]	No. of Discharge Cycles	Testing Period (hr)
24	1.2	0.10	1.5	0.65	0.066	0.10	0.108	0.38	10	108
L-4	1.0	0.13	1.5	0.42	0.055	0.083	0.085	0.48	4	29
34	0.3	0.05	1.6	1.0	0.05	0.08	0.11	0.19	8	56
43	0.9	0.09	1.0	0.92	0.082	0.082	0.076	0.33	3	8
45	0.8	0.09	1.0	1.0	0.09	0.10	0.071	0.33	3	30
48	0.4	0.17	0.8	0.65	0.11	0.09	0.043	0.63	1	8

[a] These values were calculated using the capacity measured for the first discharge.

[b] The 1-hour rate is nominally 0.27 A/cm^2.

Table 5, (continued)

Cell No.	Purpose of Experiment	Results
24	Test 56.7 wt % Se - 43.3 wt % Te cathode mixture.	Paste cracked terminating the test; product build-up at paste-current collector interface; 500°C required for capacity measurement shown.
L-4	Test 30 wt % Se - 70 wt % Te cathode mixture at 400°C.	No cathode material found at paste-anode interface; severe corrosion of low-carbon steel housing and current collectors by Te and the formation of nonconducting products terminated test.
34	Test 87.7 wt % Se, 8.9 wt % P, and 3.4 wt % Li_2Se cathode mixture contacted with LiF-LiCl-LiI eutectic at 500°C.	Reproducible performance for 2 days and 6 cycles; 500°C required for performance shown; no Li_2Se at paste-anode interface.
43	Test 36.7 wt % Se - 63.3 wt % Tl cathode mixture at 400°C.	No cathode material found at paste-anode interface; build-up of product between cathode mesh-paste interface cracked paste resulting in shorted cell; more open structure allowing convection of product from paste interface appears to be needed.
45	Test 23.9 wt % S - 76.1 wt % Tl cathode mixture.	Same as for Cell No. 43.
48	Test cell similar to Cell No. 45 in vertical position at 400°C (compared to 465°C for Cell No. 45) and with a more open cathode structure.	No cathode material found at paste-anode interface; paste cracked due to insufficient support for paste.

All of the cathode mixtures tested showed lower capacity densitites than selenium cathodes in the present cell design. A major aim in the additive investigation, therefore, is to determine the minimum quantity of additive that will eliminate cathode material transfer to the anode and will also cause the smallest decrease in capacity density. A detailed description of several of the cells shown in Table 5 is presented below in Sections (e) to (h).

As shown in Table 1, 28 lithium/chalcogen cells were tested during this reporting period. Of these, the nine cell tests discussed below in Sections (a) to (h) contributed to understanding the problem of cathode-material transfer to the anode. The remaining cell tests made other contributions to improving cell performance such as cell design changes required for sealing the various cathode mixtures and means of preventing paste cracking due to insufficient support, buildup of products at the cathode-paste interface, or too high spring loading forces. Those cells discussed in detail typically indicated the limitations of the various types of paste electrolytes and those additives which were successful in eliminating cathode-material transport to the anode. A summary of the remaining cells tested is presented in the appendix.

(a) Tests Results for Cells No. 27, 39, and 40

The objective of Cells No. 39 and 40 was to determine the selenium permeability rate of modified infiltrated paste electrolytes fabricated by pressing a salt-poor filler disk of $LiAlO_2$ and LiF-LiCl-LiI eutectic with subsequent infiltration of additional electrolyte. Selenium permeability measurements of a totally infiltrated paste electrolyte, prepared by pressing a $LiAlO_2$ filler disk with subsequent infiltration of all of the LiF-LiCl-LiI electrolyte to fill the pores of this disk, indicated that approximately 10 wt % of the selenium loaded into the cathode was transferred to the anode in 40 hours (Cell No. L-6 in Table 4). Further attempts to prepare totally infiltrated disks were hampered by frequent cracking of the disk during infiltration. Modified infiltrated disks were used in subsequent tests because of easier fabrication (few losses due to disk cracking during infiltration). The helium permeability of the best disks prepared using both techniques was approximately 0.1 ml He min^{-1} cm^{-2} at 1 atm differential pressure.

The results from Cells No. 39 and 40 indicated that the modified infiltrated paste electrolyte has a much higher selenium transport rate than that measured for the totally infiltrated paste electrolyte with no electrical performance measurements. Performance measurements for Cells No. 39 and 40 are shown in Figs. 4 and 5. The cells performed well during the first 8 hr of testing, but then performances decreased sharply after a 16-hr period on open circuit. As shown by Figs. 4 and 5, performances of thse cells were similar

Fig. 4. Voltage-Capacity Density Discharge Curves for Lithium/Selenium Cells No. 27, 39, and 40 (electrode area, 31.6 cm^2; temperature, 380°C; numbers on curves indicate discharge cycle numbers).

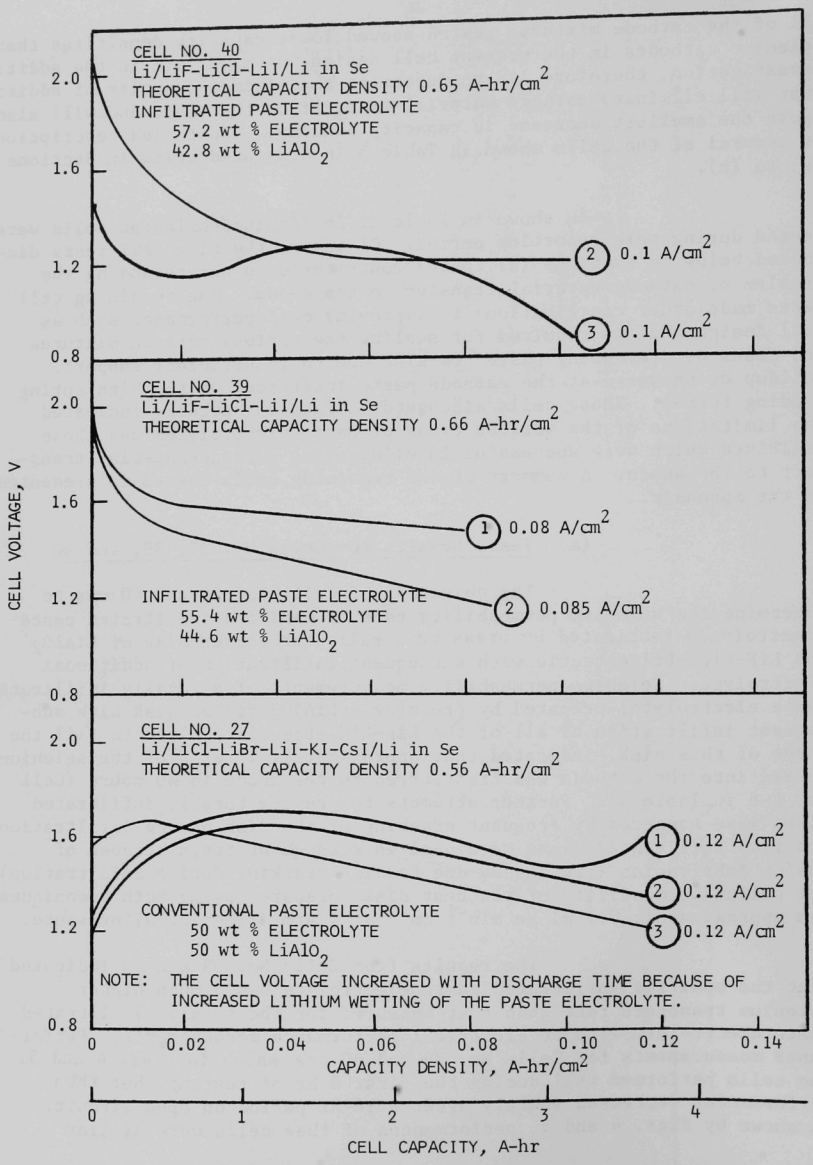

Fig. 5. Voltage-Capacity Density Charge Curves for Lithium/Selenium Cells No. 27, 39, and 40 (electrode area, 31.6 cm^2; temperature, 380°C; numbers on curves indicate charge cycles).

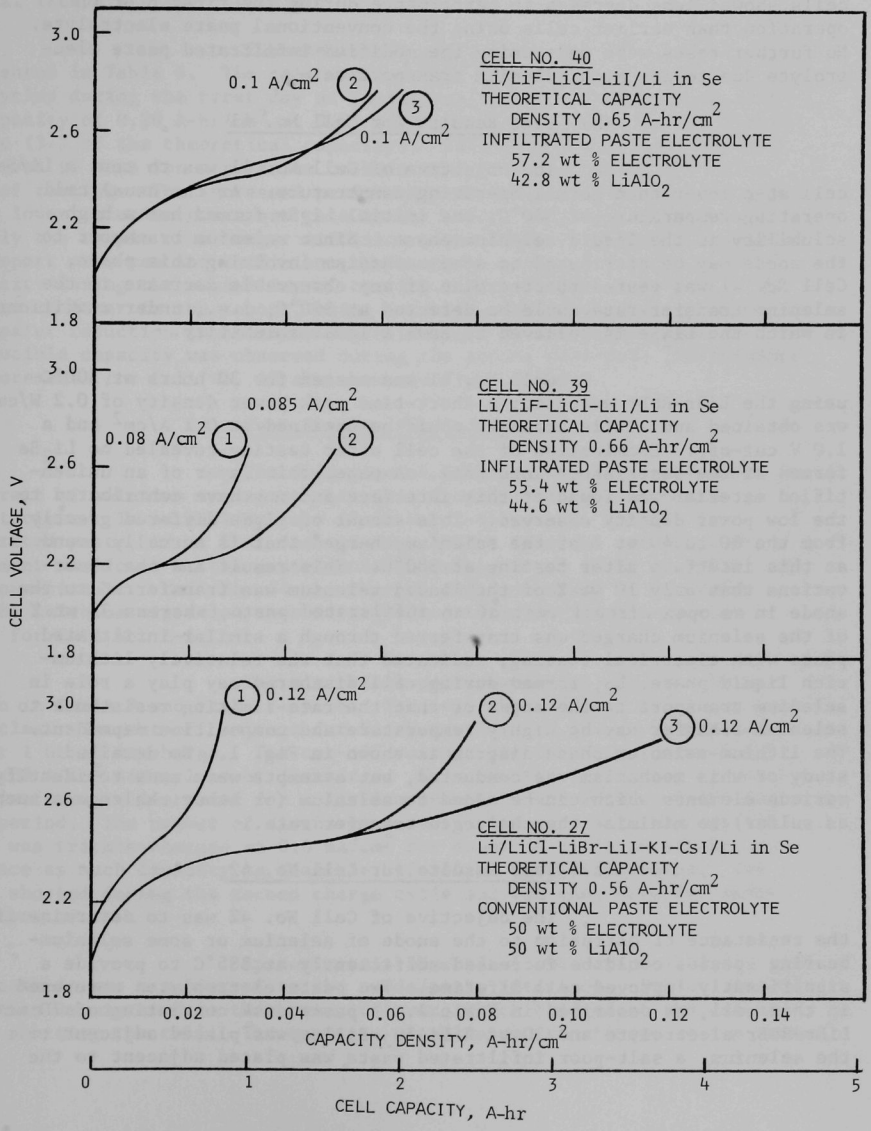

to that of Cell No. 27 (see Table 1) in which a conventional paste electrolyte was infiltrated in the cell. The performance of these cells showed less decrease in performance during the first 8 hr of operation than earlier cells using the conventional paste electrolyte. No further tests were made using the modified infiltrated paste electrolyte due to its high selenium transport rate.

(b) Test Results for Cell No. 41

The objective of Cell No. 41 was to test a Li/Se cell at a lower than normal operating temperature. At the usual cell operating temperature of 380°C, the initial Li_2Se formed has a high solubility in the liquid selenium phase. Since selenium transport to the anode may be attributed to some mechanism involving this phase, Cell No. 41 was tested to determine if any observable decrease in the selenium transfer rate could be detected at 300°C, i.e., under conditions in which the Li_2Se is believed to have a lower solubility.

Cell No. 41 was tested for 30 hours at 300°C using the LiBr-RbBr eutectic; a short-time peak power density of 0.2 W/cm^2 was obtained and little capacity could be obtained at 0.1 A/cm^2 and a 1.0 V cut-off. Examination of the cell after testing revealed no Li_2Se formed at the paste/anode interface. A paper-thin layer of an unidentified material was found at this interface and may have contributed to the low power density observed. This amount of Li_2Se differed greatly from the 30 to 40 wt % of the selenium charged that is normally found at this interface after testing at 380°C. This result and the observations that only 10 wt % of the loaded selenium was transferred to the anode in an open-circuit test of an infiltrated paste, whereas 38 wt % of the selenium charged was transferred through a similar infiltrated paste with electrical testing, indicated that the relatively lithium-rich liquid phase, L_2, formed during cell discharge may play a role in selenium transport to the anode or that the rate-limiting resistance to selenium transfer may be highly temperature and composition dependent. The lithium-selenium phase diagram is shown in Fig. 1. No detailed study of this mechanism was conducted, but attempts were made to identify various elements which can be added to selenium (or other chalcogens such as sulfur) to minimize the chalcogen transfer rate.

(c) Test Results for Cell No. 42

The objective of Cell No. 42 was to determine if the resistance of diffusion to the anode of selenium or some selenium-bearing species could be increased sufficiently at 385°C to provide a significantly improved cell lifetime. Two paste electrolytes were used in this cell, as described in Table 1. A paste disk consisting of 70 wt % LiBr-RbBr electrolyte and 30 wt % $LiAlO_2$ filler was placed adjacent to the selenium, a salt-poor infiltrated paste was placed adjacent to the

lithium, and the assembled sections were clamped together. The interelectrode distance for this cell was 0.52 cm, approximately twice the normal interelectrode distance.

The electrical performance for Cell No. 42 is presented in Table 6. The cell was operated for 56 hr and 7 cycles (4 cycles during the first day at increasingly higher current densities). A capacity of 0.20 A-hr/cm^2 at 0.25 A/cm^2 was demonstrated on the fourth cycle (37% of the theoretical capacity). This is the best performance achieved to date for a selenium cathode over 4 cycles during the first day of testing. The increased performance observed is probably the result of a lower selenium transport rate to the anode, which might have been merely the result of a longer diffusion path. This reduction of selenium transport rate was not sufficient, however, to maintain a reproducible capacity during the second day of testing. The results of Cell No. 44, discussed later in the report, using a totally infiltrated paste showed a greater reduction in selenium migration rate to the extent that reproducible capacity was observed during the second test day. Performance measurements for Cell No. 42 are shown in Figs. 6 and 7.

(d) Test Results for Cell No. 44

The objective of Cell No. 44 was to determine the rate of selenium transport through a totally infiltrated paste electrolyte. In an earlier test (Cell No. L-6) using a totally infiltrated paste, 10 wt % of the selenium loaded into the cathode compartment was found at the paste/anode interface after 40 hr at 380°C on open-circuit. Cell No. 44 was charged and discharged to determine if the selenium migration rate during electrical testing was greater than for Cell No. L-6.

The electrical performance for Cell No. 44 is shown in Table 7 and Figs. 7 and 8. The cell was operated for 40 hr and 2 cycles. The cut-off voltage for Discharge 1 was 1.1 V at 0.08 A/cm^2 after 1 hr of discharge. The cut-off voltage for Discharge 2 was 1.6 V at 0.08 A/cm^2 after 1 hr of discharge. This was the first test in which the performance increased for a lithium/selenium cell after a 24-hr testing period. The number of discharge measurements was small because the cell was trickle-charged at 0.6 mA/cm^2 for about 16 hr in an attempt to replace as much capacity as feasible before the second discharge. The cell shorted during the second charge cycle and was shut down for examination.

Approximately 38 wt % of the selenium loaded into the cathode was transferred to the anode/paste interface. Either lithium or selenium migrated in this product layer, which bridged to the cathode cup, shorting the cell. The quantity of selenium transferred to the anode

Table 6. Electrical Testing of Cell No. 42

Cell Operation	Current Density (A/cm^2)	Cut-Off Voltage[a] (V)	Capacity Density ($A\text{-}hr/cm^2$)	Fraction of Cell Capacity	Open-Circuit Voltage After Discharge/Charge Meas. (V)	Test Day
Discharge	0.042	1.84	0.042	0.07	2.04	1
Charge 1	0.042	2.28	-----	----	----	
	0.023		-----	----	----	
	0.015		-----	----	----	
	0.008		0.018[b]	0.03	2.12	
Discharge 2	0.082	1.67	0.082	0.14	2.04	
Charge 2	0.082	2.28	-----	----	----	
	0.051		-----	----	----	
	0.026		0.052[b]	0.09	2.04	
Discharge 3	0.17	1.32	0.17	0.30	2.00	
Charge 3	0.17	2.28	0.15	0.27	2.04	
Discharge 4	0.25	0.40	0.20	0.37	2.00	
Charge 4	0.10	2.24	0.11	0.22	----	2
	0.057	2.28	----	----	----	
	0.028		0.014[b]	----	2.12	
Discharge 5	0.17	0.64	0.06	0.15	2.02	
Charge 5	0.17	2.28	0.05	0.11	----	
	0.057		----	----	----	
	0.019		0.015[b]	0.03	2.14	
Discharge 6	0.11	0.4	0.061	0.13	----	
Charge 6	0.11	2.28	0.041	0.09	2.08	

Trickle charge for 16 hr at 2.2 mA/cm^2.

[a] Cut-off voltage for discharge was the IR-included voltage. Cut-off voltage for charge was the IR-free voltage.

[b] This fraction of theoretical capacity is the sum of all fractions not shown for the charge or discharge.

Fig. 6. Voltage-Capacity Density Curves for Lithium/Selenium Cell No. 42.

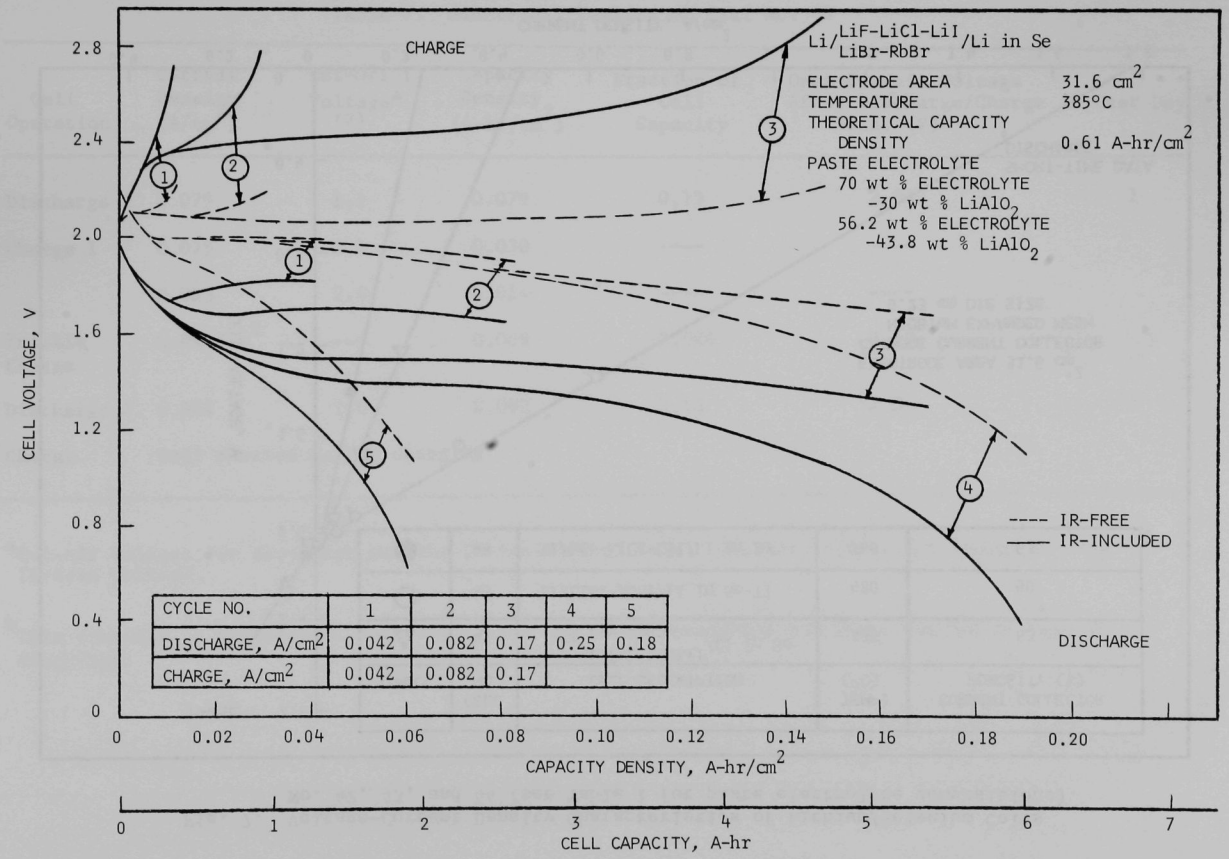

CYCLE NO.	1	2	3	4	5
DISCHARGE, A/cm²	0.042	0.082	0.17	0.25	0.18
CHARGE, A/cm²	0.042	0.082	0.17		

Fig. 7. Voltage-Current Density Characteristics of Lithium/Selenium Cells No. 42, 43, and 44 (see Table 1 for paste electrolyte compositions).

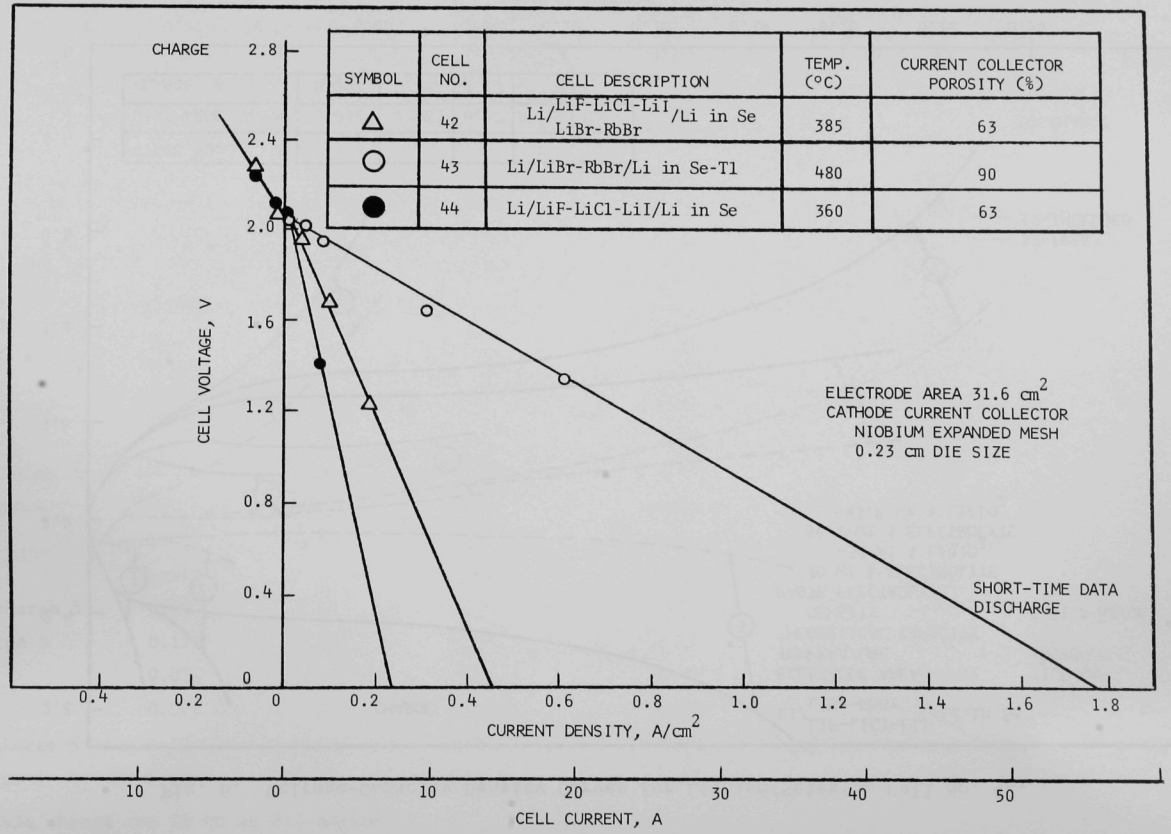

SYMBOL	CELL NO.	CELL DESCRIPTION	TEMP. (°C)	CURRENT COLLECTOR POROSITY (%)
△	42	Li/LiF-LiCl-LiI, LiBr-RbBr/Li in Se	385	63
○	43	Li/LiBr-RbBr/Li in Se-Tl	480	90
●	44	Li/LiF-LiCl-LiI/Li in Se	360	63

Table 7. Electrical Testing of Cell No. 44

Cell Operation	Current Density (A/cm^2)	Cut-Off Voltage[a] (V)	Capacity Density ($A\text{-}hr/cm^2$)	Fraction of Cell Capacity	Open-Circuit Voltage After Discharge/Charge Meas. (V)	Test Day
Discharge 1	0.079	1.1	0.079	0.13	2.04	1
Charge 1	0.079	2.1	0.030	----	----	
	0.023	2.4	0.014	----	----	
Trickle Charge	$0.6 mA/cm^2$	---	0.009	0.084	2.12	
Discharge 2	0.082	1.6	0.082	0.14	2.06	2
Charge	Cell shorted during charging.					

[a]Cut-off voltage for discharge was the IR-included voltage. Cut-off voltage for charge was the IR-free voltage.

[b]This fraction of theoretical capacity is the sum of all fractions not shown for the charge or discharge.

Fig. 8. Voltage-Capacity Density Curves for Lithium/Selenium Cell No. 44.

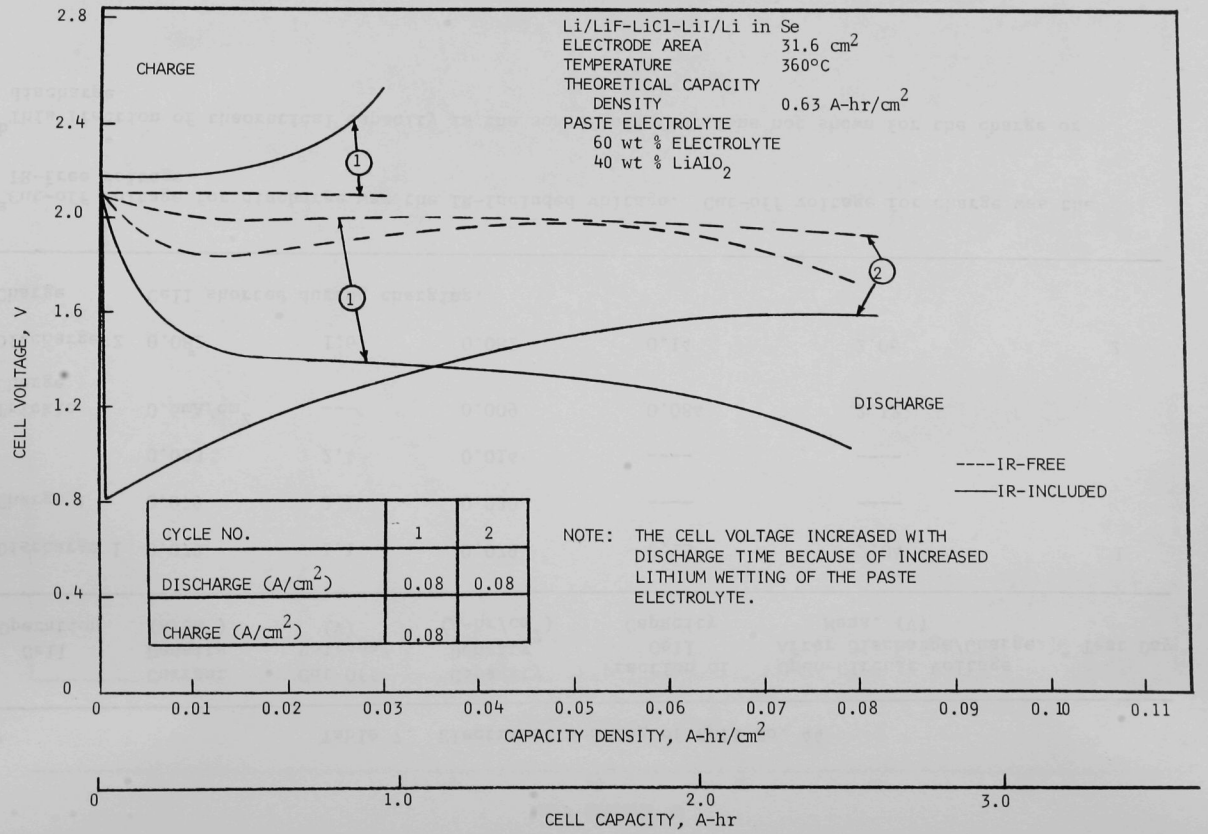

is considerably higher than the 10 wt % transferred in the absence of electrical testing for Cell No. L-6. It appears at this point that the lithium-rich liquid phase, L_2, formed during discharge may play a role in the transport of selenium to the anode. The most effective means of eliminating the selenium migration in paste electrolytes appeared at this point to be the addition of suitable materials to selenium.

(e) Test Results for Cell No. 34

The objective of Cell No. 34 was to test the effect of phosphorus addition to the cathode on selenium permeability of the paste electrolyte. The cathode composition was 87.7 wt % Se, 8.9 wt % P and 3.4 wt % Li_2Se saturated with LiF-LiCl-LiI eutectic at 500°C. The cell was tested for 56 hr and 8 cycles. The short-time peak power density was 0.3 W/cm^2. The capacity density measured for cycles 2 and 6 at 0.05 A/cm^2 on the first and second test days was 0.04 A-hr/cm^2. Although this selenium-phosphorus cathode mixture showed promise of delivering reproducible performance, a redesign of the cell would be necessary to overcome the low capacity and power density achieved using the present cell design. Cells using viscous electrolyte and a porous metal current collector would decrease the cell resistance and may give greater cathode material utilization.

(f) Test Results for Cell No. 43

The objective of Cell No. 43 was to test the effect of thallium addition to the cathode on the selenium transport rate to the anode. Thallium is of interest as an additive since it is expected that its lower electrical resistivity should provide higher peak power densities than the phosphorus mixture discussed above. It was surmised that the problem of low power density with phosphorus-selenium or phosphorus-sulfur mixtures could be reduced by redesigning the cell (such as using a design containing liquid electrolyte and no paste), but the goal of this portion of the investigation was to find an additive which (1) eliminated selenium transport through the paste, (2) had a minimum negative effect on the capacity presently achievable in Li/Se cells, and (3) required a minimum amount of redesign of the cell components.

The cathode composition for Cell No. 43 was 36.7 wt % Se - 63.3 wt % Tl (60 at. % Se, 40 at. % Tl). The electrical performance of this cell is presented in Figs. 7 and 9. The phase diagrams[4] for the Li-Tl and Se-Tl systems are shown in Fig. 10. The short-time peak power density was approximately 1.0 W/cm^2. The capacity measurements indicated that the diffusion overvoltage was large; therefore, attempts were made to increase the capacity in later cells by using a less elaborate current collector thereby allowing more rapid diffusion of the products from the paste/cathode interface to take place. The

Fig. 9. Voltage-Capacity Density Curves for Lithium/Selenium-Thallium Cell No. 43.

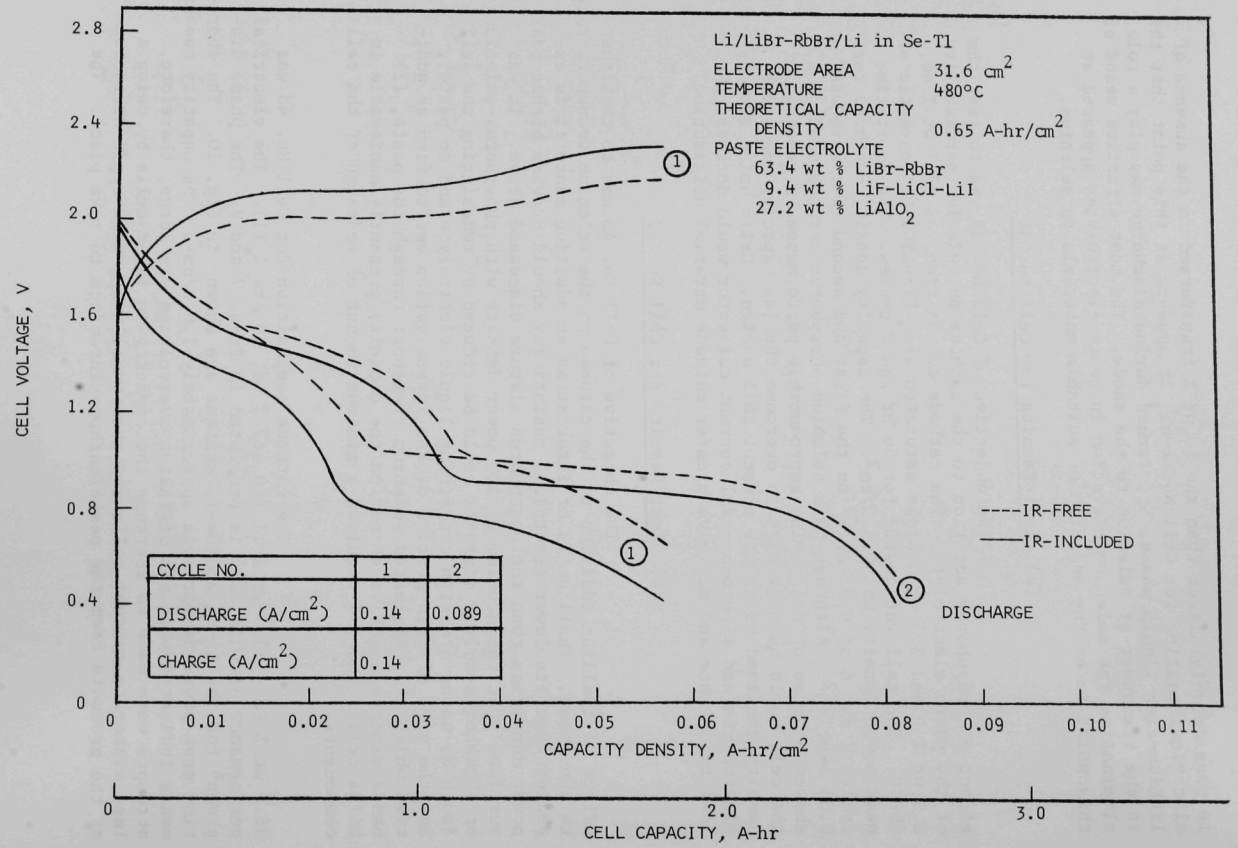

Fig. 10. Phase Diagrams for Selenium-Thallium and Lithium-Thallium Systems. (From *Constitution of Binary Alloys*, 2nd ed., by M. Hansen and K. Anderko. Copyright 1958 by McGraw-Hill Book Co. Used with permission of McGraw-Hill Book Co.)

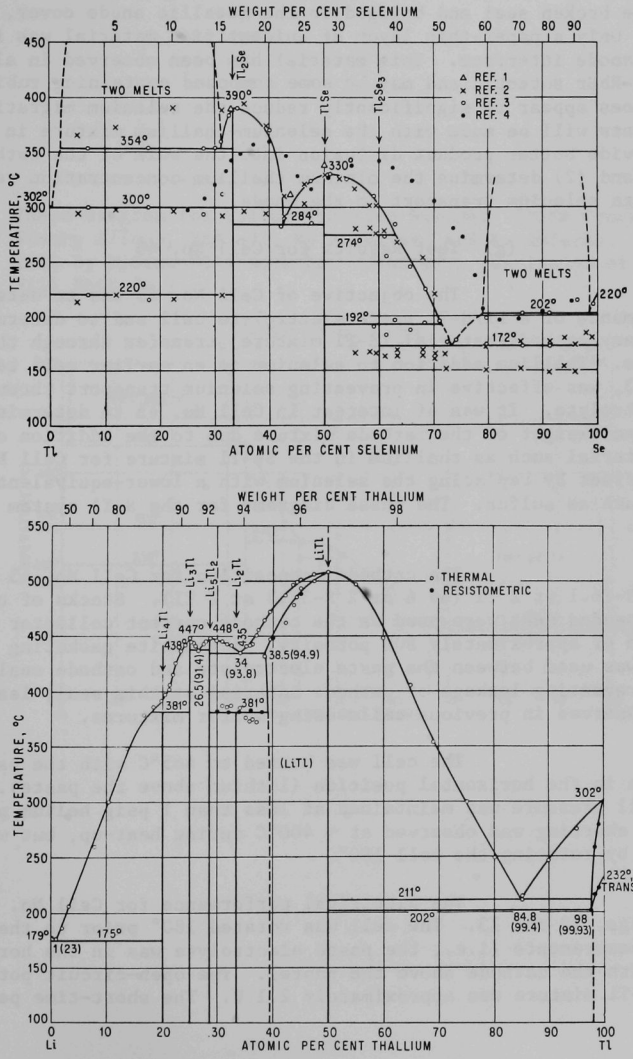

cell was tested for 8 hr after which time electrical shorting was observed. Examination of the cell after disassembly indicated that the product had not readily diffused through the mesh adjacent to the paste, causing the accummulation of a product layer 3 mm thick which forced the paste away from the cathode sealing surface. Some of the liquid cathode alloy leaked through the broken seal and bridged to the metallic anode cover, shorting the cell. Only a paper-thin layer of unidentified material was found at the paste/anode interface. This material has been observed in all cells using LiBr-RbBr eutectic and may be some compound containing rubidium. Thallium does appear to significantly reduce the selenium migration rate. Further tests will be made with the selenium-thallium mixture in order to (1) provide better product diffusion into the bulk of the cathode material, and (2) determine the minimum thallium concentration required to eliminate selenium transport to the anode.

(g) Test Results for Cell No. 45

The objective of Cell No. 45 was to determine the performance of a Li/S-Tl paste electrolyte cell and to determine if there was any cathode-material (S-Tl mixture) transfer through the paste electrolyte. Thallium addition to selenium in an earlier cell test, Cell No. 43, was effective in preventing selenium transport through the paste electrolyte. It was of interest in Cell No. 45 to determine if the increased weight of the cathode mixture due to the addition of a high-density material such as thallium in the Se-Tl mixture for Cell No. 43 could be offset by replacing the selenium with a lower-equivalent-weight material such as sulfur. The phase diagram[4] for the S-Tl system is shown in Fig. 11.

The cathode composition for Cell No. 45 was 23.9 wt % S-76.1 wt % Tl (66.6 at % S-33.3 at % Tl). Stacks of corrugated niobium expanded mesh were used as the cathode current collector to form a structure of approximately 80% porosity. A graphite gasketing material (Grafoil) was used between the paste electrolyte and cathode sealing surface, preventing leakage of cathode material at this seal; leakage had been observed in previous cells using sulfur mixtures.

The cell was heated to 465°C with the paste electrolyte in the horizontal position (lithium above the paste). The furnace well pressure was maintained at less than 1 psig helium pressure. Electrical shorting was observed at $\sim$ 400°C during heat-up, but was eliminated by rotating the cell 180°.

The electrical performance for Cell No. 45 is shown in Figs. 12 and 13. The cell was rotated 180° prior to the performance measurements (i.e., the paste electrolyte was in the horizontal position with the cathode above the paste). The open-circuit potential for this S-Tl mixture was approximately 2.1 V. The short-time peak power

Fig. 11. Phase Diagram for Sulfur-Thallium System. (From *Constitution of Binary Alloys*, 2nd ed., by M. Hansen and K. Anderko. Copyright 1958 by McGraw-Hill Book Co. Used with permission of McGraw-Hill Book Co.)

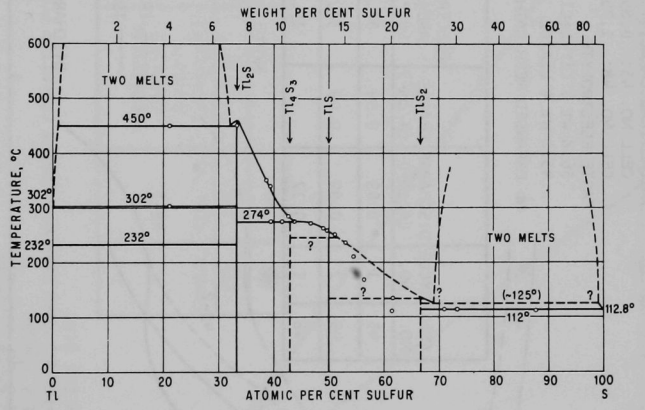

Fig. 12. Voltage-Capacity Density Curves for Lithium/Sulfur-Thallium Cells No. 45 and 48.

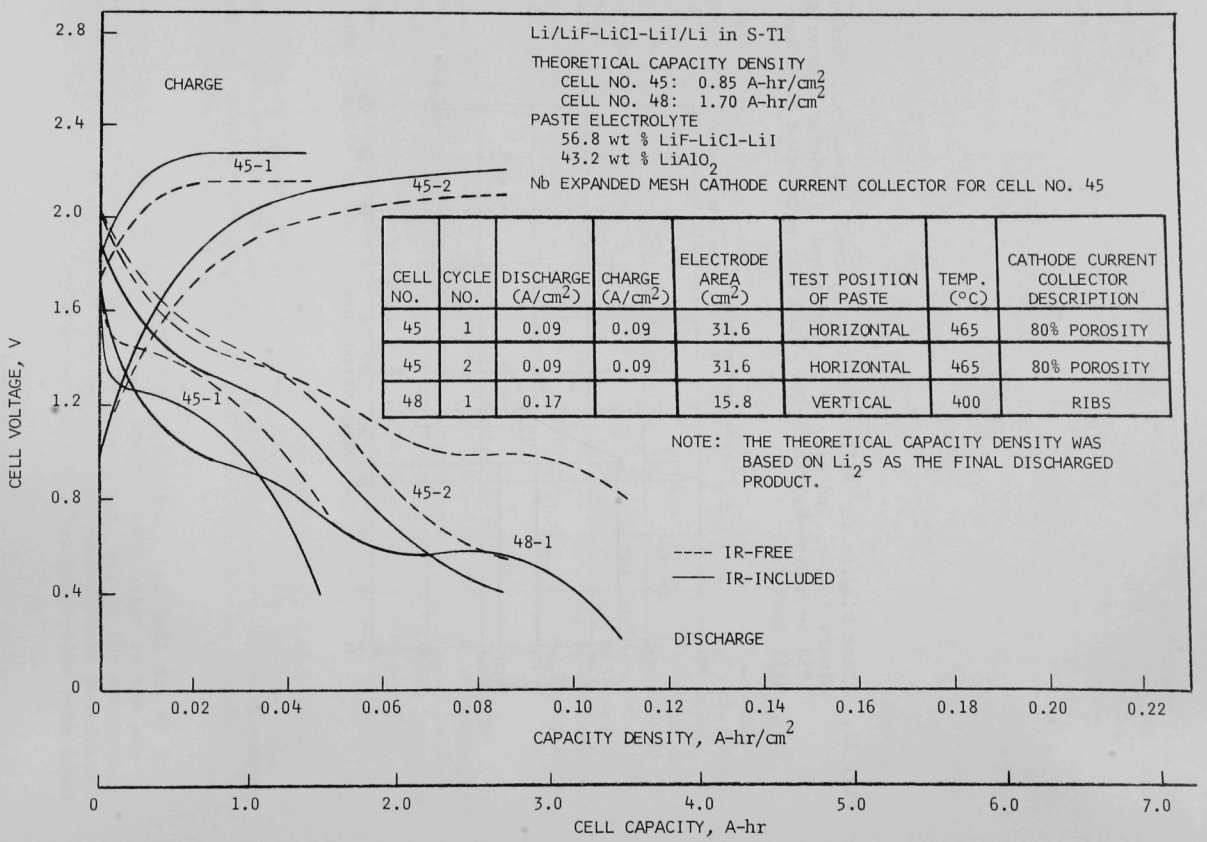

CELL NO.	CYCLE NO.	DISCHARGE (A/cm^2)	CHARGE (A/cm^2)	ELECTRODE AREA (cm^2)	TEST POSITION OF PASTE	TEMP. (°C)	CATHODE CURRENT COLLECTOR DESCRIPTION
45	1	0.09	0.09	31.6	HORIZONTAL	465	80% POROSITY
45	2	0.09	0.09	31.6	HORIZONTAL	465	80% POROSITY
48	1	0.17		15.8	VERTICAL	400	RIBS

Fig. 13. Voltage-Current Density Characteristics of Lithium/Sulfur-Thallium Cells No. 45 and 48.

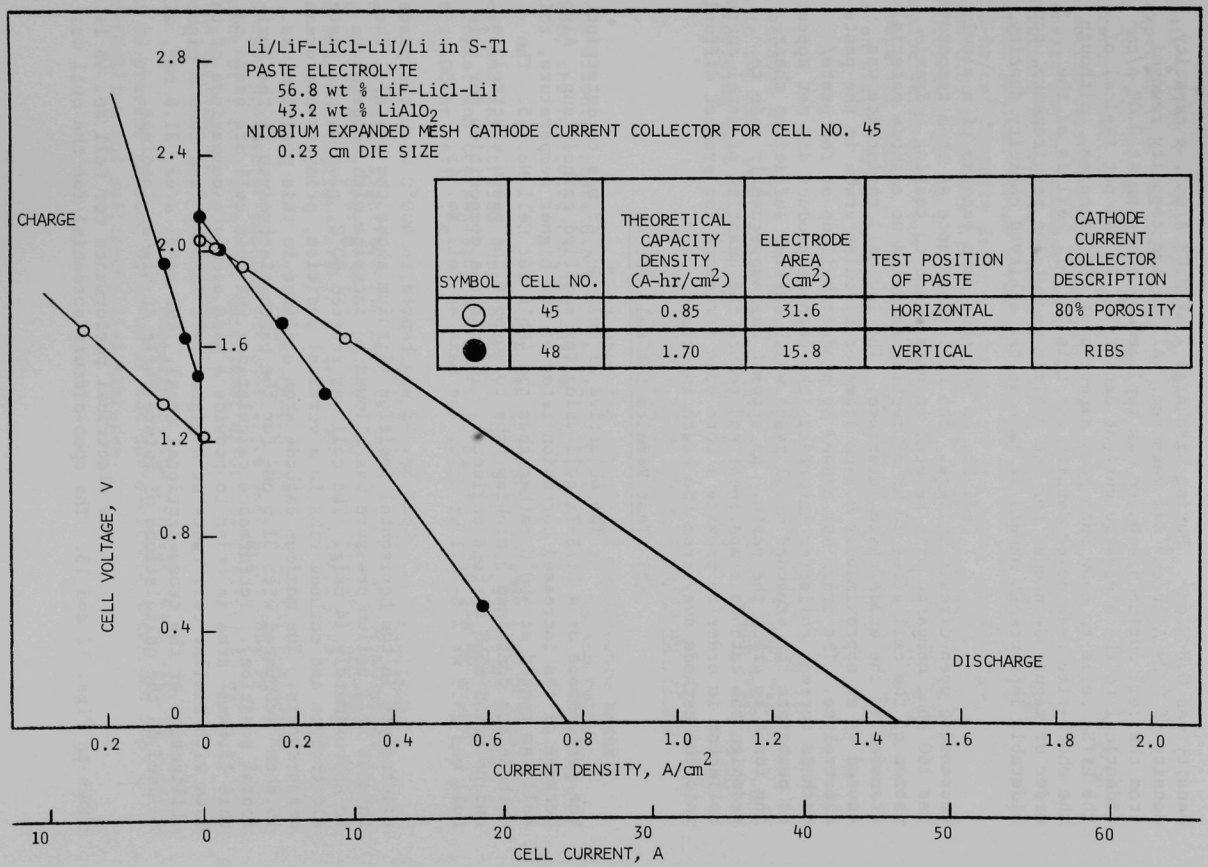

SYMBOL	CELL NO.	THEORETICAL CAPACITY DENSITY (A-hr/cm^2)	ELECTRODE AREA (cm^2)	TEST POSITION OF PASTE	CATHODE CURRENT COLLECTOR DESCRIPTION
○	45	0.85	31.6	HORIZONTAL	80% POROSITY
●	48	1.70	15.8	VERTICAL	RIBS

density was 0.8 W/cm^2. During Discharge 2 at 0.09 A/cm^2, a capacity density of 0.09 A-hr/cm^2 was measured. All of the capacity removed from the cell during discharge was replaced by charging at 0.09 A/cm^2 (identical to the discharge current density). It was not typical of the Li/Se cells to show such good ampere-hour efficiencies. Although the short-time peak power density for this Li/S-Tl cell is of the order of magnitude needed for the vehicle propulsion requirements, considerable improvement should be made in the achieved capacity density.

Cell No. 45 was shut down because of a slowly decreasing open-circuit voltage. The cell resistance at room temperature was 160 ohms compared with several megohms prior to testing. Examination of the cell after 30 hr of testing revealed no cathode material transfer to the anode/paste interface. The low cell resistance was caused by an approximately 6.3-cm diameter circular crack in the paste electrolyte. The crack was caused by product buildup at the paste/cathode current collector interface (the cathode product did not appear to penetrate the expanded metal mesh) which exerted sufficient shearing force to crack the paste. An attempt was subsequently made to redesign the cathode compartment and reduce the quantity of metal current collector in order to provide a more open structure for product diffusion into the cathode away from the paste interface.

(h) Test Results for Cell No. 48

The objective of Cell No. 48 was to determine the performance of a Li/S-Tl cell using the modified cathode cup. Also, because of the increased corrosion rates at the higher temperature, this cell was tested at 400°C rather than the 465°C for Cell No. 45. The cathode cup contained 5 niobium ribs to support the paste electrolyte, and no metal mesh current collector. The cathode composition for this cell was 23.9 wt % S-76.1 wt % Tl, the same as Cell No. 45.

Cell No. 48 was heated to 400°C with the paste electrolyte in the horizontal position (lithium above the paste). The furnace well helium pressure was allowed to increase with temperature to approximately 14 psig. The cell was rotated 90°C, placing the paste electrolyte and cathode ribs in a vertical position, prior to performance measurements. The maximum cathode area utilized in this position was 15.8 cm^2 (compared with 31.6 cm^2 for the paste electrolyte in the horizontal position). Performance calculations for this cell are based on this 15.8-cm^2 area in order to provide a more accurate comparison of these data with similar cell tests at a higher S-Tl loading (and thus a higher utilization of the cross-sectional area). The total area, 31.6 cm^2, will be used in the calculations of future cells at higher loadings.

The electrical performance for Cell No. 48 is shown in Figs. 12 and 13. The open-circuit potential for the cell was

approximately 2.16 V. The short-time peak power density was 0.4 W/cm^2. It was expected that the peak power density would be lower than that observed for Cell No. 45 since Cell No. 48 did not contain a niobium mesh current collector. If a cell of this type performs well and satisfies other electric vehicle propulsion requirements such as cycle life, the power density may be increased by using techniques to provide better lithium wetting of the paste electrolytes or possibly by using higher-salt-content pastes. These areas may require future investigations. The 0.1 A-hr/cm^2 capacity density achieved at the lower temperature, 400°C, and 0.09 A/cm^2 was slightly higher than that measured for Cell No. 45, 0.09 A-hr/cm^2 to a 0.4 V cut-off. Further tests will be made to determine which paste position (horizontal or vertical) yields the highest capacity density. The cathode-material loading will be doubled and an even higher value is expected for the capacity density at 0.09 A/cm^2.

Cell No. 48 was shut down after 8 hr of testing because of a crack in the paste electrolyte. An attempt will be made in the next cell tested to decrease the chance of paste cracking by providing more support for the paste electrolyte.

(i) Conclusions from Tests of Cells No. 23 to No. 48 and L-4 to L-6

Based upon the electrical performance tests for 7.5-cm diameter paste electrolyte Cells No. 23 to No. 48 and Cells L-4 to L-6, the following conclusions can be drawn:

1) Selenium transport through conventional, salt-poor, and infiltrated paste electrolytes is the life-limiting factor for the cells, and the selenium transport of all of these pastes is too high for a 100-hr cell life.

2) Phosphorus, tellurium, and thallium addition to selenium significantly reduces the rate of cathode-material transfer to the anode over a 30-hr period. Sulfur-thallium mixtures showed a behavior similar to that of selenium-thallium mixtures.

3) Selenium-thallium and sulfur-thallium mixtures show promise of meeting the short-time peak power density requirement of 1 to 3 W/cm^2 but additional effort is required to increase the utilization in these cells.

4) Redesign of the present cells will be required to prevent product build-up at the paste-cathode interface for selenium-thallium and sulfur-thallium mixtures.

5) Additional effort is required (1) to determine the minimum thallium concentration required for Se-Tl and S-Tl alloys to prevent cathode-material transfer to the anode and (2) to develop cells with mixed cathodes which perform as well as lithium/selenium cells in terms of power density and capacity density.

B. Life Testing and Charge-Discharge Cycle Testing of Lithium/Chalcogen Cells

No report for this period.

C. Design of High-Specific-Power Lithium/Chalcogen Cells

No report for this period.

D. Automatic Charge-Discharge Testing of Multiple Lithium/Chalcogen Cells

No report for this period.

TASK 2. PASTE ELECTROLYTE STUDIES
(L. E. Trevorrow and J. G. Riha)

The properties of the paste electrolyte are considered to be important factors in the performance of lithium/selenium cells. The observed permeability of paste electrolytes to gaseous helium has been interpreted as an indication of mechanical imperfections that contribute to the interelectrode leakage of selenium. Therefore, the development of pastes with minimum permeability has been assumed to be a requirement for the successful use of rigid paste electrolytes in cells. This section describes the recent experimental effort devoted to the development of procedures for the fabrication of paste disks possessing low permeability to helium and to the production of a number of disks to be used in electrical cell tests.

The previous report[1] described the use of helium flow measurements as a means of determining the factors in paste fabrication procedures that significantly affected the permeability of paste electrolye disks. This earlier work showed that fabrication conditions can be chosen to reduce the porosity of a paste disk of 1.3-cm diameter and 0.25-cm thickness to the point that the leak rate of gaseous helium at 25°C and also at 400°C is equal to or less than 3 ml min^{-1} atm^{-1} cm^{-2}. These conventional paste electrolytes were fabricated by pressing a mixture of filler and salt that had been repeatedly pulverized and heated above the electrolyte melting point. Also, those paste disks fabricated by the infiltration technique indicated even lower helium permeability (less than 0.04 ml min^{-1} atm^{-1} cm^{-2}). The infiltrated paste electrolytes were fabricated by allowing molten salt to soak into disks previously pressed from powdered lithium aluminate. The infiltration technique had been initiated because of the following rationalization: Disk strength contributed by surface-tension forces probably cannot be fully realized unless filler particles are in contact and joined by a liquid bridge.[5] It was assumed that this physical situation might be approached best by first pressing a disk of filler, to establish particle-to-particle contact, and then adding sufficient molten salt to just fill the interparticulate voids.

Because of the low permeability exhibited by 1.3-cm diameter disks prepared by infiltration, the major effort of the recent 6-month period has been concerned with developing procedures for the preparation of 7.5-cm diameter disks by infiltration. Work with 7.5-cm diameter disks was preferred because their larger area affords more

sensitive tests of permeability, their fabrication and handling is more likely to uncover problems associated with paste disks of the size currently being used in cells, and disks with promising permeability characteristics can be used in equipment currently employed in cell tests.

Although 1.3-cm diameter disks had been readily prepared by infiltration of pure filler disks, the first efforts to prepare 7.5-cm diameter disks were unsuccessful because the disks cracked during the infiltration process. Tantram *et al.*[6] described similar difficulties in the preparation of paste electrolytes for molten carbonate fuel cells. They found that cakes pressed from pure, powdered MgO cracked during infiltration by molten alkali carbonates. They were successful, however, in the infiltration of cakes pressed from a mixture of filler and salt that contained less than the required total amount of salt. We have found that an adaptation of this latter technique, in which cakes were pressed from a mixture of filler and about 60% of the required total salt and then infiltrated, resulted in the successful preparation of 7.5-cm disks. Several such disks were prepared and used both in helium permeability tests and in cell tests (Task 1, Section A). If the rationalization concerning disk strength (described above) holds any truth, however, the pressing of salt-filler mixtures, even with low salt content, might prevent the establishment of contact between filler particles. Therefore, an additional effort to prepare 7.5-cm diameter disks by the infiltration of pure filler cakes was continued with alteration of fabrication conditions until a set of conditions was found that resulted in disks that were intact.

Since the present procedure has resulted in preparation of several 7.5-cm diameter electrolyte disks by infiltration of pure filler without cracking, it appears to be suitable for routine application. Therefore, the set of conditions used, all of which are sufficient but perhaps not necessary, are described below in detail.

Disks were pressed from pure filler powder as follows: About 16.5 g of lithium aluminate powder (< 100 mesh, 56 m^2/g) that had been dried at 300-500°C in a flowing helium stream was loaded into the mold shown in Fig. 14. Leveling of powder in the mold was very important for obtaining a disk with parallel faces. The powder surface was first leveled with a spatula. A loose-fitting ram was then hand-pressed onto the powder surface and removed. The impression of the ram on the powder surface was inspected to detect low spots which were then filled with powder. This leveling and inspection procedure was repeated until the powder surface appeared to be planar. The top ram was put into place, the mold was evacuated to 10^{-2} Torr and heated to 150°C, and a pressure of 500 kg/cm^2 was applied to the rams for 1 hr using a hydraulic press located in a helium-atmosphere dry box. (The pressure at which the filler disk was pressed was critical to the preparation of intact disks; pure filler disks pressed at higher pressures,

Fig. 14. Cross Section of Mold Used to Press 7.5-cm Diameter Disks from Powdered Lithium Aluminate.

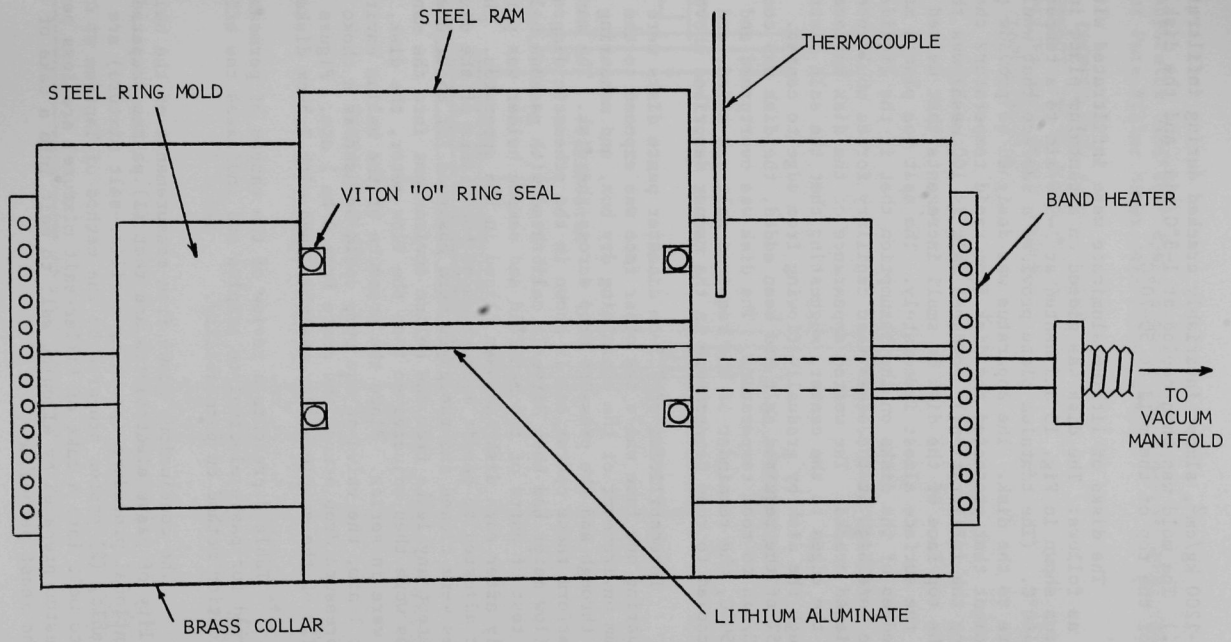

1000-1200 kg/cm^2, almost invariably cracked during infiltration by molten salt.) The mold was then cooled at 1-3°C/min, and the disk was pushed out of the top of the mold at 50-70°C.

The disks of lithium aluminate were infiltrated with molten salt as follows: The disk was placed on a tantalum plate in the apparatus shown in Fig. 15 and heated at 1-3°C/min to a temperature of 450-460°C. (The tantalum plate provided a surface that would not adhere to the disk. The apparatus was designed to provide an environment that protected the disk from rapid temperature changes during the infiltration.) Powdered salt (< 100 mesh) was then added to the top face of the disk in small increments that melted and soaked into the surface almost immediately. The salt was placed mainly at the edges of the disks on the assumption that if the liquid/filler ratio were high at the edges then capillary forces would prevent edge-initiated cracks. The wetted appearance of the disk surface spread from the edges to the center, suggesting that the salt distributed through the disk by gradually flowing from edge to center. After about 60-75% of the required salt had been added, the disk was cooled at 1-3°C/min to room temperature. The disk was overturned and reheated to 450°C, the remainder of the required salt was added, and the disk was cooled to room temperature in the manner described above.

Permeabilities of 7.5-cm diameter paste disks were measured by evacuating one face while the other face was exposed to the gaseous helium environment of the containing dry box, and measuring both the flow rate through and the pressure drop across the disk. The manifold used to perform these operations is shown in the schematic diagram of Fig. 16. The flow meter had been directly calibrated with gaseous helium. A leak test of parts of the manifold and sample holder was performed initially after each disk had been placed in the apparatus. The valves were first adjusted to permit evacuation of both faces of the disk, then all valves were closed and the gages were observed for about one-half hour to detect any leaks from the helium environment into the manifold. The valves were then adjusted so that the flow meter, the disk, and the pump were in series. Since the pressure of the helium environment was about 1 atm, the valve at the pump could be used as a choke to adjust the pressure drop across the paste from 0 to 1 atm. Figure 17 shows details of the sample holder assembly used with 7.5-cm disks.

Table 8 presents a review of the ranges of permeability observed for paste electrolyte samples and indicates the effect of the fabrication method on permeability.

The conclusions drawn from measurements of the helium permeability of paste electrolytes are that (1) pastes prepared by the conventional procedure (pressing a filler-salt mixture) are the most permeable, (2) pastes prepared by the method of Tantram *et al.* (allowing salt to melt into a cake of filler-salt mixture) are less permeable, and (3) pastes prepared by allowing salt to melt into a cake of pure filler are the least permeable.

Fig. 15. Apparatus Used to Prepare Electrolyte Disks by Infiltration of Pure Filler Disks with Molten Salt.

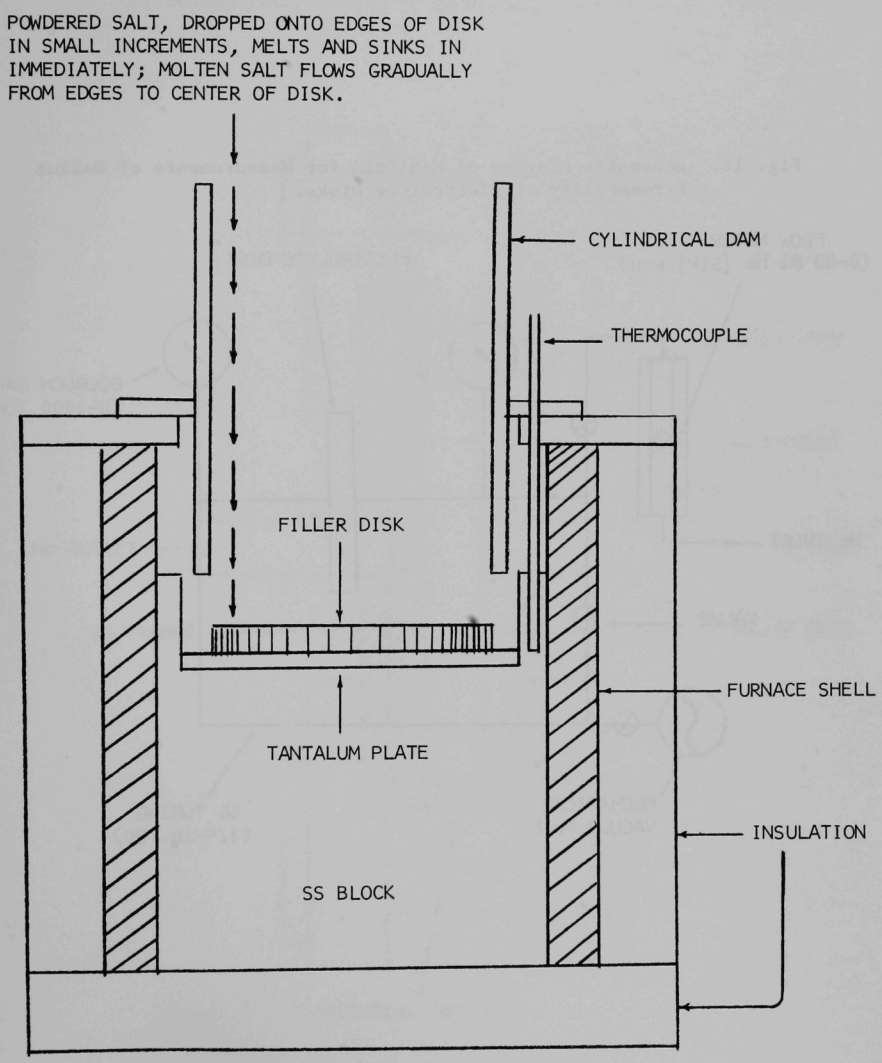

Fig. 16. Schematic Diagram of Manifold for Measurements of Helium Permeability of Electrolyte Disks.

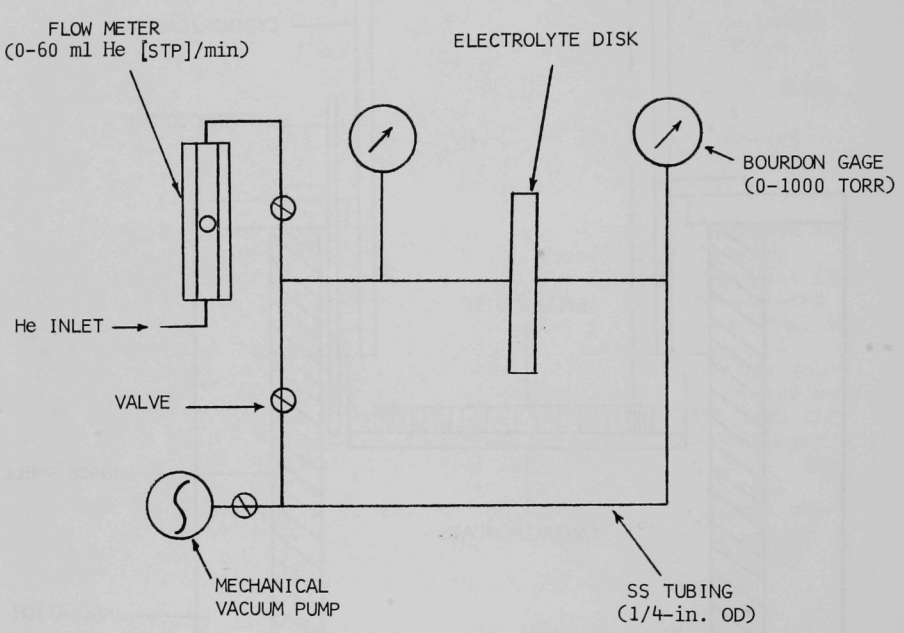

Fig. 17. Cross-Sectional Representation of Sample Holder for Measurements of Helium Permeability of Electrolyte Disks at Room Temperature.

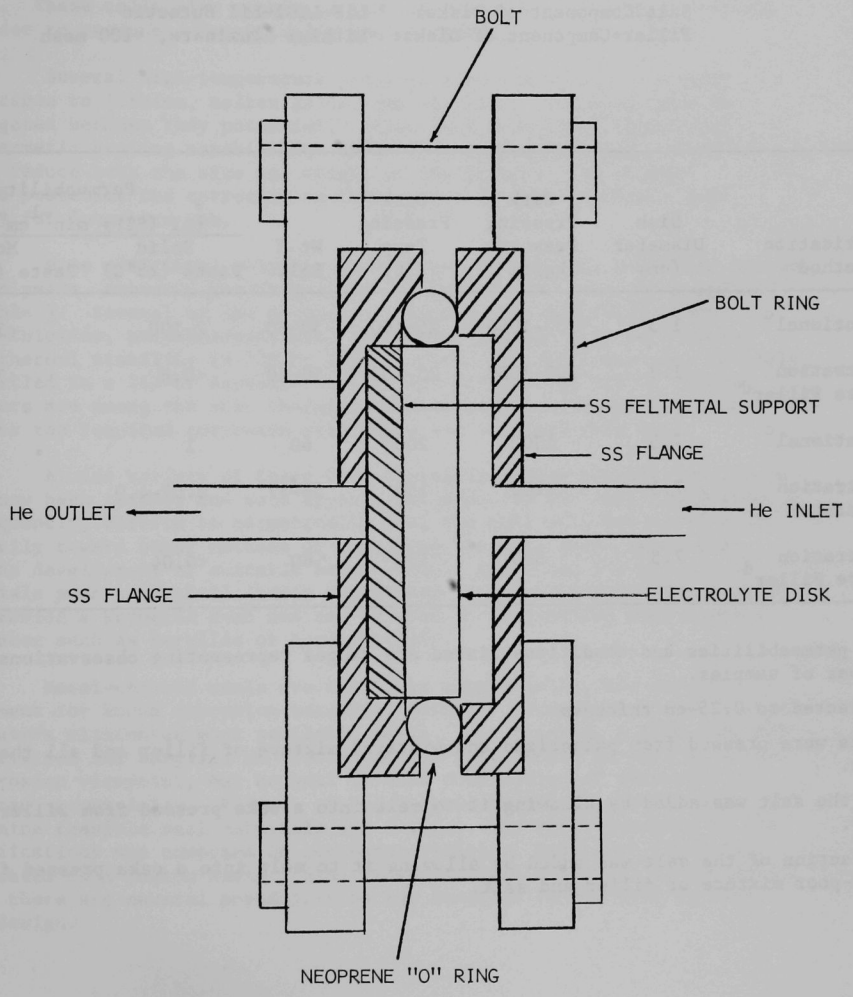

Table 8. Review of the Effect of Fabrication Method on the Helium Permeability of Electrolyte Disks[a]

Salt Component of Disks: LiF-LiCl-LiI Eutectic
Filler Component of Disks: Lithium Aluminate, <100 mesh

Fabrication Method	Disk Diameter (cm)	Disk Pressing Pressure (kg/cm^2)	Disk Pressing Temp (°C)	Wt % Salt	Permeability[b] [ml (STP) $min^{-1} cm^{-2} atm^{-1}$]	
					Solid Paste (25°C)	Molten Paste (370-400°C)
Conventional[c]	1.3	700-1050	25-100	50-60	2-100	<3-30
Infiltration of Pure Filler[d]	1.3	700-1050	25-100	50-60	<0.8	<3
Conventional[c]	7.5	1300	200	60	1	--
Infiltration of Mixture[e]	7.5	1200	150	56-57	0.09-4.0	--
Infiltration of Pure Filler[d]	7.5	600	150	~60	<0.04	--

[a] The permeabilities and conditions listed are ranges representing observations on a number of samples.

[b] Corrected to 0.25-cm thickness.

[c] Disks were pressed from pulverized and sintered mixture of filler and all the required salt.

[d] All the salt was added by allowing it to melt into a cake pressed from filler powder only.

[e] A fraction of the salt was added by allowing it to melt into a cake pressed from a salt-poor mixture of filler and salt.

TASK 3. SEALANTS AND INSULATORS
(M. L. Kyle and F. J. Martino)

Lithium/selenium cells require electrically-insulating materials resistant to lithium, selenium, lithium-selenium alloys, and molten halide salts. These cells also require a sealant resistant to these conditions in order to produce a hermetically sealed battery.

Several high-temperature polymers were tested for corrosion resistance to lithium, molten salts, and selenium. Polymers were investigated because they potentially offer both electrical insulating and hermetic sealing capabilities in a thin, lightweight form which could reduce both the size and weight of the battery. No polymer tested possesses the corrosion resistance and thermal stability necessary for long-term use.

Nine additional polymers were tested during this reporting period. The polymers, exposure conditions and results of the tests are presented in Table 9. Several of the polymers, including the benzimidazobenzophenanthioline, polybenzimidazole, and hydrophenazine polymers, showed good thermal stability in 125-hr argon exposure at 380°C but were severely embrittled in a 113-hr exposure to LiF-LiCl-LiI salt at 375°C. These polymers are among the most thermally stable polymers tested but appear to lack the required corrosion resistance for internal cell use.

A wide variety of these more thermally stable pliable insulators have now been tested, and none appears satisfactory for cell application. Consequently, efforts to hermetically seal the cell will now be directed primarily toward other methods of providing hermetic seals, especially (1) the development of suitable metal-ceramic seals and (2) the use of materials such as Grafoil (resin and binder-free graphite packing) which can provide a hermetic seal and can be used in conjunction with a solid insulator such as beryllia or boron nitride.

Metal-ceramic seals are available commercially, but our requirement for known corrosion-resistant metallic conductors and electrical insulators eliminates most available seals. For example, a seal composed of beryllium and beryllia or niobium and beryllia would be desirable from a corrosion viewpoint, but no seal in this combination of materials is produced commercially. Vendors of these seals have been contacted to determine feasible seal materials and designs, and seals designed to our specifications and composed of corrosion-resistant materials could be fabricated on a custom basis. Some leeway in seal materials is available since there are several possibilities for location of the seal in the cell design.

Table 9. Stability of Insulating Polymers

Polymer	Condition After 125-hr Exposure to Argon at 380°C	Condition After 113-hr Exposure to LiF-LiCl-LiI Eutectic Salt at 375°C
M-BBB-2[a]	Unaffected	Brittle
BBL-SN-2[a]	Brittle	Not tested
BBB-33-1-C[a,b]	Unaffected	Brittle
Polybenzimidazole[c]	Unaffected	Failed
Hydrophenazine[c]	Unaffected	Brittle, cracked
P-11-E, Polypyrrolone[c]	10 % weight loss	Brittle, cracked
Diphenyl Ether Polyimide	Failed	Not tested
DuPont XP Perfluorosulfonic Acid	Failed	Not tested
Chemstrand TR-BX-2-ICO (Developmental)	Failed	Not tested

[a] Benzimidazobenzophenanthroline polymers cast from CH_3SO_3H obtained from Dr. R. L. Van Deusen, Air Force Materials Laboratory, Wright-Patterson Air Force Base, Ohio.

[b] Yarn drawn at 575°C.

[c] Samples obtained from Dr. Donald H. White, The University of Arizona.

TASK 4. CORROSION BY LITHIUM/SELENIUM MIXTURES

(M. L. Kyle and F. J. Martino)

The development of reliable, long-lived lithium/selenium secondary batteries requires corrosion-resistant materials. Selenium, lithium, and the molten salts utilized in these cells are relatively reactive and consequently are corrosive to many common materials. The selection of suitable corrosion-resistant materials is a major requirement for the successful utilization of these batteries.

Corrosion of metallic conductors by molten lithium is not being extensively investigated at the present time because the containment of lithium and current collection from it can probably be done with austenitic stainless steels or similar conventional materials. These steels have performed well in laboratory tests for several hundred hours.

Current emphasis is on the cathode compartment, which requires a material resistant to the selenium and lithium-selenium alloys that are present in the cathode compartment in the partially discharged state. Most corrosion tests are performed with a 20 at. % lithium-selenium mixture, which was chosen as representative of the cathode composition of a partially discharged cell. A lithium-selenium alloy, rather than pure selenium, is used in the corrosion program because of the observation that synergistic corrosive effects may occur in lithium-selenium alloys. The presence of lithium precludes containment of lithium-selenium alloys in any metal whose primary corrosion resistance is obtained as the result of an oxide surface film. Consequently, the corrosion testing of potential cell containment materials is done under approximate cell operating conditions.

Most corrosion tests reported to date have been of 200-350 hr duration and indicated the possible usefulness of several materials including beryllium, niobium, niobium - 1% zirconium alloy, chromium, Unitemp 605, Haynes 25, and aluminum. The annual corrosion rates reported were obtained by measurements of the amount of corrosion that occurred during the test and linear extrapolation to an annual rate. An annual rate is useful for comparing materials that have been tested for different lengths of time.

The results of 600-hr tests confirmed the observed low corrosion rates for aluminum, beryllium, and chromium. Higher corrosion rates were observed for niobium, niobium-1% zirconium alloy, Unitemp 605, and Haynes 25. A difference in corrosion rates was observed between two lots of beryllium with different BeO contents. Beryllium containing about 1 wt % BeO demonstrated a corrosion rate of 0.014 mm/yr while a higher (2 wt %) BeO-content beryllium was attacked at a rate of about 1.0 mm/yr. Figure 18 presents the results of both long and short-term corrosion tests of the more corrosion-resistant materials.

Fig. 18. Corrosion Rates Observed in 20 at. % Li-Se Mixtures (temperature, 375°C; dynamic isothermal capsule tests).

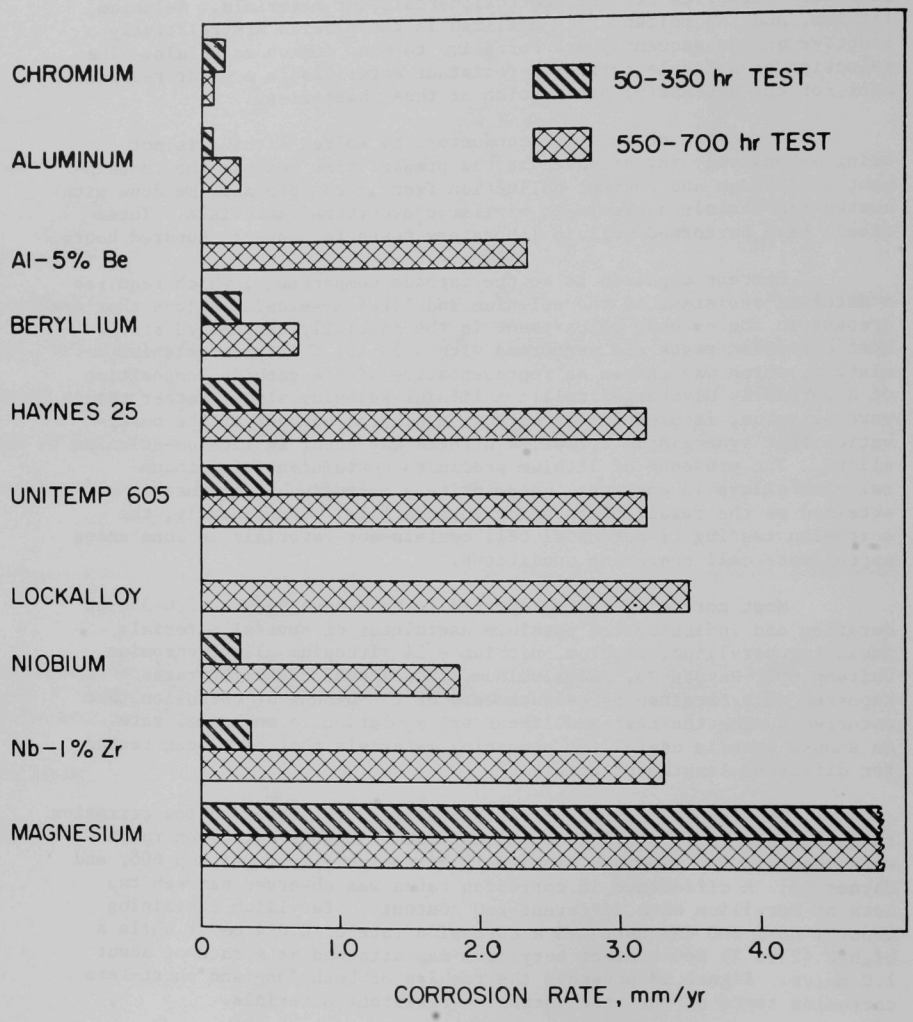

A beryllium foil (3.5×10^{-2} mm thick) sample containing 0.02% BeO was exposed to a Se-20 at. % Li mixture for 113 hr at 375°C. At the conclusion of the test, the sample could not be located in the melt. If this reacted completely, the corrosion rate would be reported as > 1.8 mm/yr. Corrosion rates of this magnitude have been observed on some beryllium samples tested. The corrosion resistance of beryllium does not appear then to be a function solely of BeO content. This sample differed from previous samples in the high degree of surface working present in the foil samples. Other samples were generally of pressed-and-sintered material (N50 grade).

Two other samples of this beryllium foil were exposed to LiF-LiCl-LiI eutectic salt and LiBr-RbBr eutectic salt for 113 hr at 375°C. The sample exposed to the LiF-LiCl-LiI was destroyed whereas the sample exposed to LiBr-RbBr was attacked at a rate of 0.59 mm/yr. These data suggest that molten salt corrosion of beryllium should be investigated further on material found to be more corrosion resistant than the foil.

The corrosion resistance of beryllium to the lithium-selenium system appears to be highly variable and not all factors affecting this variability are known at this time. A more thorough study of beryllium purity, surface finish, and oxide content may be required to establish those factors affecting beryllium corrosion.

Chromium has consistently demonstrated good corrosion resistance to lithium-selenium mixtures. An additional sample was exposed to a Se-20 at. % Li mixture for 550 hr at 375°C. After test, the sample evidenced a corrosion rate of 0.02 mm/yr and was found to be electrically conductive. This result is consistent with previous long (600-hr) and short (100-300 hr) term tests. Since chromium has consistently withstood attack by lithium-selenium systems, it may be a better choice for use in construction of those cells to be used in initial life tests than is beryllium. Chromium is difficult to fabricate but housings could be constructed by chromium plating other materials, such as steels. Current collectors, however, would be more difficult to construct, since geometries of this type are difficult to plate directly and might have to be produced by plating of the stock material before the current-collector structure is formed.

TASK 5. LITHIUM/CHALCOGEN BATTERY STUDIES

No report for this period.

CONCLUSIONS

The following conclusions can be drawn from the electrical performance tests for 7.5-cm diameter paste electrolyte Cells No. 23 to 48 and Cells L-4 to L-6:

1) Selenium permeability of conventional, salt-poor, and infiltrated paste electrolytes is the life-limiting factor for the cells, and the selenium permeability of those pastes is too high for a 100-hour cell life.

2) Phosphorus, tellurium, and thallium addition to selenium significantly reduces the rate of cathode-material transfer to the anode. Sulfur-thallium mixtures showed a behavior similar to that of selenium-thallium mixtures.

3) Selenium-thallium and sulfur-thallium mixtures show promise of meeting the short-time peak power density requirement of 1 to 3 W/cm^2, but additional effort is required to increase the capacity in these cells.

4) Redesign of the present cells will be required to prevent product build-up at the paste-cathode interface for selenium-thallium and sulfur-thallium mixtures.

5) Additional effort is required (1) to determine the minimum thallium concentration required for Se-Tl and S-Tl cells to prevent cathode-material transfer to the anode, and (2) to develop cells with mixed cathodes which perform as well as lithium/selenium cells in terms of power density and capacity density.

The conclusions drawn from helium permeability measurements of paste electrolytes are that pastes prepared by the conventional procedure are most permeable, pastes prepared by the salt-poor procedure are less permeable, and infiltrated pastes are least permeable.

The materials testing results indicated that chromium, aluminum, and beryllium are the most corrosion-resistant materials tested in the Li-Se alloys at 375°C in 600-hr tests. Chromium has consistently performed well with corrosion rates of < 0.15 mm/yr (6 mpy). Aluminum has exhibited corrosion rates from 0.01 to 0.4 mm/yr, and beryllium corrosion rates have ranged from 0.01 to > 1.8 mm/yr.

FUTURE WORK

The above investigations have shown that thallium addition to selenium and sulfur significantly reduces the cathode material transfer rate to the anode. These cathode mixtures also show promise of meeting

the short-time peak power density requirement of 1 to 3 W/cm^2. Therefore, investigations in the next six-month period will include (1) efforts to develop selenium-thallium and sulfur-thallium cells which perform as well as lithium/selenium cells in terms of power density and capacity density, and (2) efforts to determine the minimum thallium concentration required for Se-Tl and S-Tl cells which show satisfactory performance for 100 hr or longer.

ACKNOWLEDGEMENT

The authors appreciate the constructive review of the manuscript by Drs. J. R. Huff, J. B. O'Sullivan, and H. J. Barger of MERDC.

APPENDIX

As shown in Table 1, 28 lithium/chalcogen cells were tested during this reporting period. Those cells not discussed previously are shown in Table 10. Results from these cells were used to make various cell changes required for better cathode sealing and changes required to prevent paste cracking due to insufficient support, build-up of products at the paste interface, or too high spring-loading forces.

Table 10. Lithium/Chalcogen Cells with 7.5-cm Diameter Paste Electrolytes

Cell No.	Purpose of Experiment	Results
23	Test the effect of using a cathode material of higher melting point than the paste electrolyte on selenium transfer to the anode. Used vertical testing position for cell.	Paste cracked; good peripheral seal; cathode mixture showed poor charging characteristics.
25	Same as Cell No. 23. Test corrosion of Be housing under cell operating conditions. Test LiCl-LiBr-LiI-KI-CsI paste electrolyte.	Evidence of Be corrosion. Some Se leaked from cell. Higher cell resistance than measured using LiF-LiCl-LiI eutectic.
26	Test horizontal start up for sealing cathode compartment. Test LiBr-RbBr paste.	No Se leakage from cathode at seal. Higher cell resistance than measured using LiF-LiCl-LiI eutectic. About 15% of Se transferred to anode.
28	Test Se permeability of LiF-LiCl-LiI paste electrolyte. No performance measurements were made. Helium flow through the electrolyte was 0.93 std cc He/min atm cm^2.	Li_2Se formation at anode; no leakage of Se at seal, paste cracked; little Se remaining in cathode.
LW-1	Test the proposed lightweight cell design and clamping method for performance and sealing, respectively.	Se lost from cell; cell shorting resulted from cathode material bridging to anode.
30	Test effect of As addition to cathode on Se permeability of paste electrolyte. The cathode composition was 54.5 wt % Se, 13.8 wt % As, and 31.7 wt % LiCl-LiBr-LiI-KI-CsI eutectic.	Paste cracked; Li_2Se formation at anode.
31	Test effect of P addition to cathode on Se permeability of paste electrolyte. The cathode composition was 52.2 wt % Se, 8.1 wt % P and 39.7 wt % LiCl-LiBr-LiI-KI-CsI.	No Li_2Se formation at anode; poor capacity, low power density.

Table 10, (continued)

Cell No.	Purpose of Experiment	Results
32	Test Se permeability of infiltrated paste electrolyte. An attempt was made to infiltrate a filler disk in an assembled cell.	Li_2Se formation at anode; ~ 40 wt % Se transferred to anode; this infiltration technique was not as successful as that for Cell L-6.
33	Test Se permeability of infiltrated paste electrolyte without electrical performance measurements.	Cell was accidentally exposed to air prior to testing (leak in the glovebox purification system) and subsequent reactions occurred degrading the lithium and electrolyte.
35	Test effect of containing Se in a porous graphite current collector (porosity such that Se wicks into the current collector) and testing the cell with the paste electrolyte above the Se.	Paste cracked due to build-up of product at p.e./graphite current collector interface.
36	Test effect of P_4S_{10} as cathode material to prevent product formation at the anode.	Poor cathode seal; cathode material deposited on cold sections of furnace well and cover.
38	Same as 36, but used a higher-salt-content p.e. in an attempt to provide better sealing of the cathode.	Poor cathode seal; P_4S_{10} deposited outside cell.
46	Test Se-Tl alloy without a current collector in an attempt to prevent product build-up at the paste interface.	Paste cracked (possibly due to spring loading).
47	Test S-Tl alloy without a current collector in an attempt to prevent product build-up at the paste interface.	Paste cracked due to spring loading on p.e.

REFERENCES

1. "Lithium/Selenium Secondary Cells for Components in Electric Vehicular Propulsion Generating Systems," Interim Technical Summary Report No. 2, Project Order No. MERDC 175-69, Project/Task/Work Unit IT 662705A012/02/042, Argonne National Laboratory, Chemical Engineering Division, Argonne, Illinois (also to be issued as ANL-7745; in press).

2. H. Shimotake and E. J. Cairns, presented at CITCE Meeting, Detroit, September 1968, Abstract No. 405; see also Extended Abstracts, p. 254 (1968).

3. Chemical Engineering Division, Argonne National Laboratory, Research Highlights, January-December 1969, report ANL-7650.

4. Constitution of Binary Alloys, 2nd ed., M. Hansen, ed., McGraw-Hill (1958).

5. H. Rumpf, "The Strength of Granules and Agglomerates," in Agglomeration, W. A. Knepper, ed., Interscience, New York (1962).

6. A. Tantram, A. Tseung, and B. Harris, Hydrocarbon Fuel Cell Technology, pp. 187-211, B. Baker, ed., Academic Press (1965).